Research Article

Phosphatidylserine (PS)-Targeting Chimeric Interferon (IFN) Fusion Proteins for Anti-Tumour Applications

Varsha Gadiyar[1], Viralkumar Davra[1,2], Rachael Pulica[1], Trevor Frederick[1], Christopher Varsanyi[1], Ahmed Aquib[1], Ziren Wang[1], Sergey Smirnov[1], Samhita Bapat[1], David Calianese[1], Alok Choudhary[3], Sergei V Kotenko[1], Raymond B. Birge[1]

1. Department of Microbiology, Biochemistry and Molecular Genetics, Cell Signaling Center, Rutgers New Jersey Medical School, Newark, United States; 2. Xencor Biologics, United States; 3. International Center for Public Health, Public Health Research Institute, Rutgers New Jersey Medical School, Newark, United States

In viable cells, membrane phospholipids are asymmetrically distributed, whereby the anionic phospholipid phosphatidylserine (PS) is localized to the inner leaflet of the plasma membrane. During apoptosis, phospholipid asymmetry collapses, and PS is externalized to the external leaflet where it serves as an "eat-me" signal for clearance through efferocytosis, which drives immune suppression. PS is also externalized on tumor endothelial cells, stromal cells, and cancer cells in the tumor microenvironment (TME), reflecting a pathophysiological state of solid cancers that function to suppress host anti-tumor immunity. Here, in an attempt to modulate the TME and induce an immunogenic immune response, we generated novel recombinant fusion proteins containing type I and type III IFNs (IFN-β-IFN-λ) fused into a single polypeptide chain separated by a short linker. The IFN-β-IFN-λ fusion proteins retain the functions of both type I and type III IFNs but show combined effects to improve biological function as well as enhance anti-tumor activities. To localize IFNs to sites of externalized PS, we next fused the IFN-β-IFN-λ chimeric protein to the PS-targeting gamma-carboxyglutamic acid-rich (Gla) and EGF domains of Gas-6, rendering the IFN biologics as PS-targeting modalities. Gas6-IFN-β-IFN-λ proteins selectively bind to PS, including apoptotic cells and live PS-positive CDC50 mutant cells. *In vivo*, Gas6-IFN-β-IFN-λ retain strong anti-tumor activities in a syngeneic model when expressed ectopically in E0771 breast cancer and B16-F10 melanoma models. These studies support the utility of first-in-class IFN fusion proteins that target the immune-stimulatory features of IFNs to the exposed PS in the TME.

 doi.org/10.32388/TMAXT9

Varsha Gadiyar and Viralkumar Davra equally contributed to this work.

Sergei V Kotenko and Raymond B. Birge laboratories contributed equally to this work.

Corresponding authors: Raymond B. Birge, birgera@njms.rutgers.edu; Sergei V Kotenko, kotenkse@njms.rutgers.edu

Introduction

Despite exciting advances in cancer immunology and immuno-therapy, particularly in the conceptualization of immune checkpoint inhibitors that target inhibitory receptors such as PD1 (Pembrolizumab/Keytruda and Nivolumab/Opdivo) and CTLA-4 (Ipilimumab/Yervoy and Tremelimumab/Imjuno), there is still a great need to identify new treatment options that target generalized epitopes in solid cancers[1][2][3]. Such therapeutic pitfalls and limitations of the checkpoint inhibitors and immune modulators are due in part to the diverse genetics in the etiologies of cancer, clonal evolution via changing mutational landscapes, tumor heterogeneity, and drug resistance[4][5]. Moreover, the microenvironments of many solid cancers also adapt and create an immune-tolerant milieu that prevents the host anti-tumor immunity benefits of checkpoint therapeutics[6][7][8][9]. In addition, the side effects and off-target autoimmunity[10] further necessitate the identification and characterization of new targets and modalities that can stimulate tumor immunity and benefit cancer patients.

Phosphatidylserine (PS) is an anionic phospholipid that is typically restricted to the inner leaflet of the plasma membrane[11]. However, in many cancer cells and stromal cells in the tumor microenvironment, PS is chronically externalized and can be used as a marker for the tumor mass as well as a target for cancer therapy[12][13][14][15][16]. Moreover, unlike protein targets and the glycocalyx, which is highly unstable due to the unique mutational landscapes and distinct N and O-linked glycosylation patterns, externalized PS and its re-localization to the outer membrane represent a stable epitope. Plasma membrane asymmetry is primarily maintained by two types of lipid transporters that include flippases and scramblases[17]. Flippases, such as the aminophospholipid translocases ATP11C and ATP11A, mediate ATP-dependent vectorial translocation of PS from the outer membrane to the cytosolic leaflet, while scramblases, such as Xkr8 and TMEM16F, facilitate ATP-independent random shuffling of the phospholipids in activated cells[17]. In recent years, the molecular mechanisms for PS externalization on apoptotic cells and during cell activation have become better understood. For example, during apoptosis,

caspase-mediated activation of the PS scramblase Xkr8 and caspase-mediated inactivation of the flippases ATP11A and ATP11C result in constitutive PS externalization[18][19][20]. On viable cells, calcium- and ATP-dependent activation of TMEM16F and P2X7 receptors leads to reversible PS externalization that can return to baseline after cell activation[21][22]. However, on diseased and stressed cells, such as in cancer and during virus infection, PS is externalized patho-physiologically by chronic activation of scramblases, which has been linked to host immune escape[12][23][24]. The rationale that continuously heightened exposed PS can drive immune escape is supported by recent studies showing that Xkr8 knockout (which prevents PS externalization) or mutation of the TMEM30A (which leads to the so-called PS-out tumors) can suppress host immune responses and drive tumor progression[12][25].

Based on these observations, many efforts have been envisioned to target externalized PS on tumors, most emblematically recombinant Annexins and PS-targeting antibodies such as Bavituximab, with solid pre-clinical success in murine models[26][27]. More recent efforts to target PS in tumors have also envisioned PS-targeting peptoids[28], antibody-drug conjugates[29], FC-Syt-drug conjugates[30] , and SAPC-DOPS[31]. While clearly meritorious, most of these strategies aim to neutralize PS, which is present at high density on the cell membrane. Moreover, most of the current PS-targeting approaches do not implement an immunogenic component, thereby limiting their ability to stimulate host immunity. In the present study, we introduce a conceptually new, first-in-class type of PS-targeting modality by fusing the PS-targeting domain of Gas6 (a GLA-EGF fusion) to a type I and type III IFN duet.

The rationale to use IFNs is based on the long-known feature that IFNs *in vivo* represent one of the prime components of host natural defense in higher metazoans against viral infections and cancer[32][33]. IFNs are divided into three families: type I, type II, and type III, based on sequence homology as well as their receptor usage and activities[34]. In humans, type II IFN includes a single member, IFN-γ, which is more divergent than type I and type III IFNs in terms of IFN structures, expression patterns, and biological actions[35]. By contrast, type I and type III IFNs are more functionally comparable; they are induced by similar pathogen-sensing pathways, activate analogous post-receptor signaling and transcriptional pathways, and regulate the expression of the identical set of IFN-stimulated genes (ISGs), the IFN signature[36][37]. At the biochemical level, all type I IFNs bind to a common heterodimeric IFNAR receptor, comprised of IFNAR1 and IFNAR2 subunits, while type III IFNs interact with a common heterodimeric IFNLR, comprised of IFNLR1 (also known as IL28RA) and IL10R2 (also known as IL10RB) [38][39][40]. While IFNAR and IFNLR share structural and biochemical elements enabling the activation of

common JAK/STAT and ISGF3 signaling and transcriptional activators by the two distinct ligand-receptor systems[41][42] in recent years, it has been shown that type I and type III IFNs target *in vivo* differential sets of cell types and tissues. In this respect, while type I IFN receptors are more ubiquitously expressed in a variety of nucleated cells, type III IFN receptors are predominantly expressed in cells lining epithelial barriers that include the respiratory, gastrointestinal, and reproductive tracts[43][44][45]. These observations indicate functional compartmentalization of the action of type I and type III IFNs and suggest that type III IFNs represent a more restricted first line of defense at sites of viral exposure as well as adenocarcinomas, while type I IFNs regulate a more robust and systemic response.

In addition to their role in antiviral immunity, both type I and type III IFNs appear to have significant anti-tumor activities[46][47]. Type I IFNs, such as IFN-α and IFN-β, can have direct effects on tumor cells by suppressing proliferation or by inducing apoptosis or necroptosis[48][49]. Type I IFNs can also act as adjuvant therapeutics to enhance anti-tumor immunity, including the polarization of macrophages towards the M1 phenotype, the activation, maturation, and enhanced cross-presentation by DCs, and the subsequent immune responses towards tumor-associated antigens, as well as direct activation of T and NK cells[50][51][52]. These features are the antithesis of what occurs in PS-positive solid tumors. Likewise, type III IFNs also appear to have anti-tumor properties and can inhibit proliferation and stimulate apoptosis of tumor cells[53][54]. Although recent studies indicate that neutrophils and DC subsets are directly responsive to type III IFNs, most immune cells do not express IFNLR1 and are not sensitive to IFN-λs. Therefore, type III IFNs might be better adapted for use as anticancer biologics as adjuvants to other immunotherapeutics, or in combination with type I IFNs. Recent studies indeed suggest that IFN-α and IFN-λ can have concerted activities to suppress certain cancers such as HCC *in vivo*[55]. A role for type III IFNs in cancer biology is further supported by findings that IFNLR knockout mice are more susceptible to sarcoma formation induced by carcinogen exposure[56]. Additionally, IFN-λ induces CXCL10 when added to mammary epithelial cells, leading to the increased recruitment of T cells to the tumor site[57]. Collectively, both type I and type III IFNs have both direct and indirect effects on tumor cells and within the tumor microenvironment.

Based on pleiotropic activities induced by type I and type III IFNs in distinct subsets of target cells in vivo, we have engineered and generated a series of recombinant IFN fusion proteins that combine type I (IFN-β) and type III (IFN-λ) IFNs into a single polypeptide chain (IFN-β-IFN-λ) to be used as broad-spectrum antiviral agents and in cancer biology. By combining IFN-β-IFN-λ into a single polypeptide with a linker, such chimeric IFNs are expected to act focally to activate immune pathways on epithelial-immune

interfaces, thereby enhancing immune outcomes. Additionally, we also fused the IFN-β-IFN-λ with the phosphatidylserine (PS) binding Gla domain of Growth Arrest Specific Factor 6 (Gas6). Gas6 and IFN-β-IFN-λ fusion protein (referred to as Gas6-IFN-β-IFN-λ throughout the paper) are developed to localize fusion proteins to regions of constitutive PS externalization. Here we present a proof-of-concept study describing a first-in-class PS-targeting modality that targets a type I and type III IFN modality with immune-oncology applications.

Material and Methods

Cell culture

Mouse triple negative breast cancer E0771 cells (CH3 Biosystems LLC), mouse melanoma B16-F10 cells, human non-small cell lung carcinoma H1299 cells, mouse lung adenoma LA4 cells, human retinal epithelium ARPE19 cells, and mouse intestine epithelium cells (mIECs) were maintained in RPMI-1640 medium (Sigma-Aldrich), HEK293T cells in DMEM medium, and CHO IFN-λR reporter cells were cultured in HAM′s F12 medium. All media were supplemented with 10% fetal bovine serum (FBS; Atlanta biologics), 100 IU/ml penicillin, and 100 μg/ml streptomycin (Sigma-Aldrich). Cells were grown at 37°C in a humidified incubator containing 5% CO_2. After thawing, cells were used for up to 8-10 passages, and their authenticities were checked by Short Tandem Repeat (STR) analysis according to the manufacturer's protocol (GenePrint 10 System, Promega). Cells were routinely checked for mycoplasma contamination.

Expression plasmids for IFN fusion proteins

Novel IFN fusion proteins were cloned into expression vectors pEF2 vector (EF-1 promoter) or pcDNA3.1 vector (CMV promoter) using infusion cloning. The fusion proteins were designed to contain a flexible linker (ASGSSGGSSGTSGSSGGSSGTST) between the IFN- and IFN-, and between the Gas6(G+E) and IFN- domains. The proteins also express a 6X His tag at the C-terminal for purification.

IFN fusion protein production. HEK293T cells were transfected with the PEF2 vector encoding various IFN or Gas6-IFN fusion expression constructs (7 μg plasmid per 10 cm plate at ~80% confluency using 28 μl LipoD293 transfection reagent). 24 hours post-transfection, the cells were washed 3 times with medium without serum and replaced with either medium alone or medium containing either 2 μg/ml vitamin K (Phytonadione injectable emulsion from Hospira) or 2 μM Warfarin (Sigma). Cell culture

supernatants containing secreted IFN proteins were collected at 72 hours post-transfection. For mock, cells were transfected with an empty vector, and cell supernatant was collected as above. Secretion of fusion molecules was confirmed by anti-His immunoblotting, as all the proteins are His-tagged.

Purified recombinant IFN fusion proteins were produced by transfecting Expi293T cells (ThermoFisher, Cat: A25869) with corresponding expression vectors. 18 hours post-transfection, cells were supplemented with 2 μg/ml vitamin K, cell culture supernatants were collected at 96 hours post-transfection, and the proteins were purified via TALON resin. 1.0 μg of purified protein was subjected to SDS-PAGE under denaturing conditions, and purity was assessed by Coomassie Blue staining.

Immunoblotting. Whole cell lysates were prepared in HNTG buffer (20 mM HEPES, pH 7.5, 150 mM NaCl, 10% glycerol) supplemented with 1% Triton X-100, 1 mM PMSF, 1 mM sodium orthovanadate, 10 mM sodium molybdate, 1 mM EDTA, 10 mM sodium fluoride, and 1% protease inhibitor cocktail. Cells were lysed, scraped, incubated on ice for 10 minutes, and centrifuged at 12,000 X rpm for 10 minutes. Cleared lysates were collected, mixed with SDS-containing Laemmli buffer, boiled for 5 minutes, and resolved by SDS-PAGE. Immunoblotting was performed with a monoclonal antibody (mAb) against either β-actin (mouse mAb; Cell Signaling, MAB374) or phospho-STAT1 (rabbit mAb; BD Bioscience, 612233) as primary Abs, followed by a secondary horseradish peroxidase (HRP)-conjugated Affinipure Goat anti-mouse Ab (Jackson ImmunoResearch, 115-035-166) or anti-rabbit Ab (Jackson ImmunoResearch, 115-035-144), respectively.

Antiviral Assay. Cells were seeded in a 96-well plate and treated with serially diluted (a one-third dilution) amounts of either recombinant murine IFN-α or IFN-λ2 or IFN-containing cell culture supernatants, starting with 100 ng of recombinant IFN proteins or 50 μl of cell supernatants in the first well in duplicates. After 18 hours of IFN treatment, vesicular stomatitis virus (VSV) was added and incubated for 24 or 48 hours, after which cells were fixed, and cell viability was determined by staining cells with 0.1% crystal violet solution followed by reading absorbance at 590 nm.

PS ELISA. 96-well ELISA plates (Greiner bio-one) were coated with L-PS (brain, porcine, Avanti Polar Lipids, Cat: 840032P and 840012) dissolved in methanol (12.5 μg/ml; 100 ml/well) by placing the plates in a sterile fume hood at 22°C until the methanol evaporated. ELISA plates were then blocked with 5% BSA in PBS overnight at 4°C. PS-coated plates were washed 3 times with lipid-wash buffer (LWB: 10 mM HEPES, 150 mM NaCl, 2.5 mM $CaCl_2$) and incubated with soluble proteins (IFN-β-IFN-λ, γ-carboxylated or non-γ-carboxylated Gas6-IFN-β-IFN-λ) diluted in 5% BSA and titrated 2-fold (the concentration range: 10 to 0.16 μg/ml) for 1 h at 22°C. Plates were then washed 3 times with LWB, and PS-bound proteins

were detected by ELISA performed with His mAb (ThermoFisher, Cat: MA1-21315; 1:1000 dilution; 1 h at 37°C) followed by alkaline phosphatase (AP)-conjugated anti-mouse IgG (Jackson ImmunoResearch, Cat: 115-055-146; 1:2000 dilution; 1 h at 37°C) and the addition of diethanolamine (DEA) buffer containing AP substrate (Sigma, Cat: S0942; 1 mg/ml). Plates were washed 3 times in PBS to remove unbound primary and secondary antibodies, and the amounts of PS-bound proteins were assessed by measuring absorbance at 405 nm over the course of 2 h.

Protection assay

96-well ELISA plates (Greiner bio-one) were coated with L-PS (brain, porcine, Avanti Polar Lipids, Cat: 840032P and 840012) dissolved in methanol (12.5 μg/ml; 100 ml/well) by placing the plates in a sterile fume hood at 22°C until the methanol evaporated. ELISA plates were then blocked with 3% BSA in Annexin V Binding Buffer for 1 hour at 37°C. PS-coated plates were washed 3 times with lipid-wash buffer (LWB: 10 mM HEPES, 150 mM NaCl, 2.5 mM $CaCl_2$) and incubated with HEK293T supernatants containing IFN-β-IFN-λ, γ-carboxylated or non-γ-carboxylated Gas6-IFN-β-IFN-λ diluted in 3% BSA and titrated 3-fold for 1 h at 37°C. Plates were then washed 3 times with LWB. mIEC cells were plated on these plates. Forty-eight hours later, after mIEC cells had adhered and formed a monolayer, VSV was added and incubated for 48 hours more. Cell viability was determined by staining cells with 0.1% crystal violet solution followed by reading absorbance at 590 nm.

Mouse experiments. Immunocompetent female or male C57BL/6 (6-8 weeks old) were obtained from Jackson Laboratory. C57BL/6 *Ifnar1*$^{-/-}$, *Ifnlr1*$^{-/-}$, *Ifnar1*$^{-/-}$*Ifnlr1*$^{-/-}$ mice, and SCID mice were bred as homozygotes at the facility. All mice were maintained in a specific pathogen-free (SPF) barrier facility, maintained under a strict 12 h light-dark cycle with access to a regular chow diet and autoclaved reverse osmosis water. For mammary tumor cell inoculation, 0.5 X 10^5 E0771 cells either mock-transfected (control cells transfected with empty plasmid), or expressing either IFN-β, IFN-λ, IFN-β-IFN-λ, Gas6(Gla)-IFN-β-IFN-λ, Gas6(Gla+EGF)-IFN-β, Gas6(Gla+EGF)-IFN-λ, or Gas6(Gla+EGF)-IFN-β-IFN-λ, or a 50:50 combination of E0771 cells expressing IFN-β and IFN-λ, or Gas6(Gla+EGF)-IFN-β and Gas6(Gla+EGF)-IFN-λ were re-suspended in RPMI-1640 complete medium containing Matrigel (50 % v/v; Corning) and injected into the 9/10 mammary fat pad of female C57BL/6 mice (n=8/group). For the melanoma model, 0.1 X 10^6 B16F10 cells either mock-transfected or expressing IFN-β-IFN-λ and Gas6(Gla+EGF)-IFN-β-IFN-λ were injected subcutaneously into the flank of male C57BL/6 mice. The tumor growth was assessed twice a week by caliper measurement of tumor diameter in the longest

dimension (*L*) and at right angles to that axis (*W*). Tumor volumes were estimated using the formula *L* X 2*W*.

The total body weight of mice was measured once a week until the end of the study. On day 29, mice were euthanized with CO_2 inhalation, and primary tumors, lungs, and spleens were collected for further analysis. Lungs were washed once in PBS and stained using Bouin solution for metastases quantification. Metastasis incidences were calculated by counting metastatic nodules in the lungs under a magnification microscope. Mouse experiments were performed in accordance with the guidelines and under the approval of the Rutgers Institutional Animal Care and Use Committee at New Jersey Medical School.

Cell Surface Binding

W3-Ildm CDC50A^{ED29} cells or calcium ionophore-treated H1299 cells (20 mM) were counted, and 5 X 10^5 cells were used for staining[58]. Cells were incubated with either HEK293T cell supernatants of fusion proteins or 20 mg/mL of purified proteins in Annexin V binding buffer at 4°C for 15 minutes. After washing, they were stained with His-PE antibody for 15 minutes. The cells were washed 3 times, and binding was analyzed by flow cytometry.

RNA sequencing

MLE-15 cells were cultured in a 6-well plate (1x10^6 cells/well) and treated (1 ng/ml) with Gas6-IFN-β-λ2 (VitK) or left untreated. RNA was collected at 7 hours using the Qiagen RNeasy Plus Mini Kit according to the manufacturer's instructions. RNA quantity and purity were assessed using a Nanodrop spectrophotometer. RNA samples were then submitted to the Rutgers Genomics Core for sequencing. RNA-Seq analysis was done in R (4.3.1). Gene set enrichment analysis was performed in R with the Bioconductor package clusterProfiler (version 3.18), where all gene ontologies (Biological Processes, Molecular Functions, Cellular Components) were included in the analysis, and the dot plot was generated with the Bioconductor package DOSE (version 2.10.6). Volcano plots were generated with the TidyVerse package ggplot2 (version 3.5.0), where significance was determined by a p-value < 0.05 and log2FC > 1 or log2FC < -1.

Statistical analysis. All *in vitro* and *in vivo* experiments were repeated at least three times. Differences between groups in all *in vivo* experiments were examined for statistical significance using a two-tailed Student's t-test and one-way ANOVA to compare multiple groups. For virus infection experiments, data were analyzed using two-way ANOVA followed by statistical significance analysis using Sidak's multiple

comparisons test for weight loss studies, and one-way ANOVA followed by statistical significance analysis using Tukey's multiple comparisons test. GraphPad Prism software was used to perform statistical analysis. $p<0.05$ was considered significant (* =$p<0.05$, ** =$p < 0.01$, *** = $p <0.001$, **** = $p < 0.0001$).

Results

Design, production, and characterization of recombinant type I/type III IFN fusion proteins. While type I and type III IFNs both activate the JAK/STAT/ISGF3 signaling pathway and induce similar sets of target genes that activate antiviral and anti-tumor immunity, expression studies indicate that type I receptors (IFNAR) and type III IFN receptors (IFNLR) are functionally compartmentalized[59]. In this capacity, type III IFN receptors are expressed on mucosal barrier-covering epithelial cells (lung, gastrointestinal, reproductive tracts), while type I IFN receptors are more ubiquitously expressed on almost all nucleated cells, the latter representing a more systemic and robust immune activation than the local activation of type III IFN receptors (**Fig.1.a.**)[59]. Here, in an attempt to improve the efficacy and targeting of IFNs, we engineered a series of recombinant fusion proteins that fuse type I IFN (IFN-β) and type III IFN (IFN-λ), separated by a linker, into a single polypeptide chain (**Fig. 1.b.**) with the goals to focally activate both Type I and Type III IFN-responding cells at immune cell/epithelial cell boundaries.

To first generate type I and type III recombinant proteins for proof-of-concept feasibility studies and to show that chimeric proteins retain functional IFN activities, DNA constructs encoding murine IFN-β, murine IFN-λ, or a murine IFN-β-IFN-λ fusion construct were cloned into a PEF2 expression vector with a C-terminal His tag, and following transfection into HEK293 cells, recombinant proteins in the culture supernatant were assayed by immunoblotting with an anti-His mAb. All proteins were produced at expected molecular weights without notable degradation (**Fig. 1.b, c.**). Subsequently, to test the *in vitro* biological activity of the proteins, we performed antiviral protection assays as illustrated in **Fig. 1.d.** For antiviral assays, we utilized 3 different cell lines depending on the expression of IFN receptors. These included mouse lung adenoma LA4 cells (that express the type I IFN receptor) (**Fig. 1.e.**), human retinal epithelium ARPE19 cells (that express both type I and type III IFN receptors) (**Fig. 1.f.)**, and mouse intestine epithelium cells (mIECs) (that express both type I and type III IFN receptors) (**Fig. 1.g.**). To demonstrate antiviral activity, the above-mentioned cells were treated with serial dilutions of IFN-containing HEK293 cell culture supernatants (**Fig. 1.d.**). After 18 h of IFN treatment, vesicular stomatitis virus (VSV) was added and incubated for 48 h, after which cells were fixed, and cell viability was

determined by staining cells with crystal violet solution followed by reading absorbance at 590 nm. The absorbance (cell viability) in the representative graphs depicts antiviral protection by IFN molecules. As expected, the LA4 cells responded only to IFN-β and IFN-β-IFN-λ (**Fig. 1.e.**), while the ARPE19 cells only responded to IFN-λ and IFN-β-IFN-λ since mouse IFN-λ but not mouse IFN-β can cross-react with human IFNLR (**Fig. 1.f.**). The mIECs responded to IFN-β, IFN-λ, and IFN-β-IFN-λ proteins **(Fig. 1.g.)**. Together, these data affirm that both IFN-β and IFN-λ moieties within the IFN-β-IFN-λ fusion protein maintain their biological activities and that the fusion molecule containing type I and type III IFN duets is stable and biologically active.

Subsequently, to test if the IFN-β-IFN-λ fusion protein displays enhanced potencies compared to IFN-β and IFN-λ given together, IEC cells were treated with equivalent amounts of IFN-β alone, IFN-λ alone, IFN-β and IFN-λ in a 1:1 ratio, and IFN-β-IFN-λ fusion protein. Twenty-four hours later, the cells were infected with VSV. Twenty-four hours after that, antiviral potency was measured by staining live cells with crystal violet. While IFN-β and IFN-λ required approximately 130 pg/mL of IFNs to show 50% activity, the IFN-β-IFN-λ fusion protein showed 50% activity at very low amounts (**Fig. 2.a.**), indicating enhanced antiviral potency when proteins are expressed as fusion proteins separated by a linker.

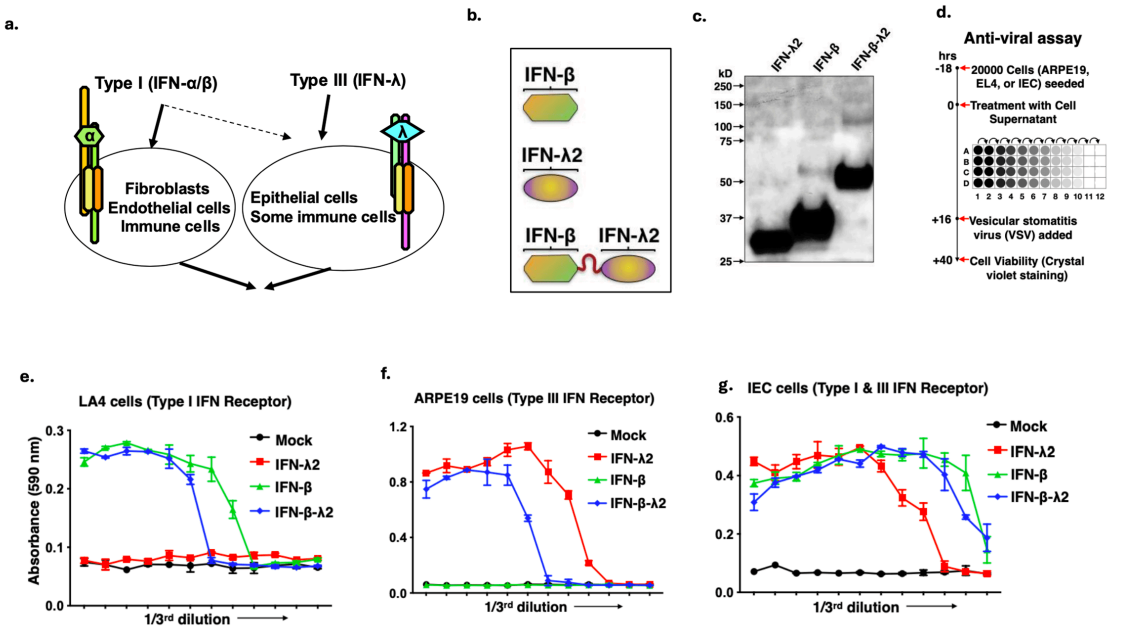


Figure 1. Design, production, and characterization of novel IFN fusion proteins. (a) The action of IFNs is compartmentalized, where type I IFNs act on fibroblasts, endothelial cells, and most immune cells, whereas type III IFNs act mainly on epithelial cells. **(b)** The schematic illustration of IFN fusion proteins.**(c)** Immunoblot showing the secretion of each protein at their expected molecular weight in the cell supernatant when probed using an anti-His antibody. **(d)** The schematic illustration depicting the antiviral assay strategy. The IFN receptor-expressing cells were pretreated with HEK293T cell supernatant containing IFN, IFN fusion, and Gas6-IFN fusion proteins. After 12 hours of pretreatment, cells were treated for 24 hours with vesicular stomatitis virus (VSV), and cell viability was determined by staining cells with 0.1% crystal violet solution followed by reading absorbance at 590 nm. **(e)** The representative graphs showing the antiviral activity of IFNs in LA4, mouse lung adenoma cells (express type I IFN receptor) **(f)**, ARPE19, the human retinal epithelium cells (respond only to mouse type III IFNs) **(g)**, and mIEC, mouse intestine epithelium cells (express both type I and type III IFN receptors).

Type I and type III IFNs have anti-tumor functions in immunocompetent syngeneic mouse models of tumor growth. To investigate the effects of IFN signaling on tumor growth *in vivo*, we used two immunocompetent mouse tumor models, the E0771 murine breast cancer model and a B16-F10 murine melanoma model. First, to assess the sensitivity of E0771 and B16-F10 cells to type I and type III IFNs, the cells were treated for 18 hours with recombinant murine IFN-α and IFN-λ2, infected with VSV, and cell viability was measured at 48 hours for E0771 cells and 24 hours for B16-F10 cells post VSV infection (**Supplementary Figure 1.a, 1.b**). Antiviral protection was observed in E0771 cells only with IFN-α but not

doi.org/10.32388/TMAXT9

with IFN-λ2, whereas both IFNs provided antiviral protection in B16-F10 cells. These data indicate that E0771 cells respond only to type I IFNs, whereas B16-F10 cells are sensitive to both type I and type III IFNs, albeit with different capabilities.

Next, to explore the anti-tumor function of IFNs and IFN fusion molecules, we generated stable transfectants of E0771 and B16-F10 cells that constitutively secrete IFNs and IFN fusion molecules (**Fig. 2b.**). No overt toxicity (apoptosis or necroptosis) in the cultured cells was observed, nor did the cells show decreased cell growth using an MTT assay (**Supplementary Figure 1.d**.). Accordingly, when ectopically IFN-secreting modified tumor cells are implanted into syngeneic mice, the tumor cell-produced IFNs act locally in the tumor microenvironment. For the *in vivo* anti-tumor studies, 0.5 X 10^5 mock-transfected E0771 cells, or E0771 cells constitutively producing IFN-β, IFN-λ, or IFN-β-IFN-λ fusion proteins were orthotopically transplanted into the mammary fat pad of C57BL/6 female mice. After tumor cell injection, tumor volume was measured twice a week and body weight once a week over the period of 4 weeks as depicted in the experimental outline **(Fig. 2c.)**. As shown in **Fig 2d-e,** both IFN-β and IFN-β-IFN-λ showed strong anti-tumor activity, while IFN-λ showed a more modest effect. As reported earlier, IFN-β has also shown an anti-tumor effect; however, strong off-target effects such as loss of hematopoiesis and ascitic fluid accumulation in the peritoneal cavity were observed (data not shown). In agreement with the data shown in **Fig. 1.g**., these data indicate that IFN-β-IFN-λ retains functional activity. This is further supported by observations that E0771 tumors grew slower in mice transplanted with the IFN-β-IFN-λ E0771 expressing cells compared to mice transplanted with 50% E0771 IFN-β cells and 50% E0771 IFN-λ cells mixed (**Fig.2.f and g**). Taken together, data in **Fig. 2f-g** support the idea that the combined action of type I and type III IFNs with the IFN fusion molecule has an enhanced capacity to modulate the local tumor microenvironment to suppress tumor growth. In addition to the marked synergistic anti-tumor activities of IFN-β-λ2, mice with tumors expressing a combination of single IFN molecules developed ascites (**Fig.2.h.)** and anemia, as suggested by the pale appearance of the liver and tumor (**Fig.2.i**), whereas mice bearing tumors expressing IFN-β-λ2 lacked these signs, potentially suggesting reduced off-target effects of the IFN-β-λ2 fusion molecules.

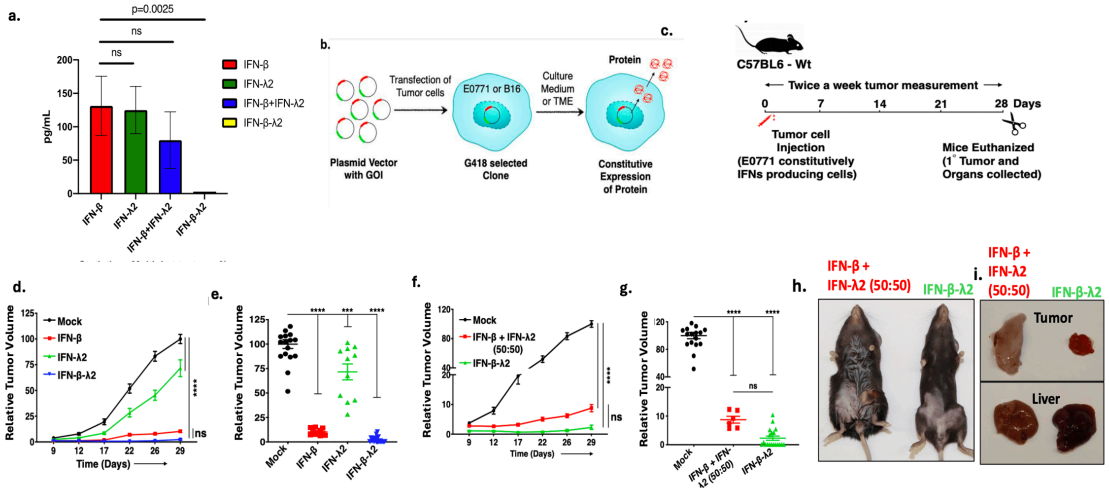


Figure 2. Type I and type III IFNs have anti-tumor functions in immunocompetent syngeneic mouse models of tumor growth. (a) Antiviral assay (VSV) at 24 h pre-treatment with equivalent amounts of IFNs on IEC cells. The concentration at which IFN treatment showed 50% activity is plotted on the Y axis (p=0.0025, n=3, multiple t-tests). **(b)**The schematic illustration showing transfection of E0771 or B16-F10 cells followed by antibiotic selection to create stable cell lines that constitutively secrete IFN fusion proteins. **(c)** The graphical illustration showing the experimental outline of the E0771 murine breast cancer tumor model in C57BL/6 mice. 5 X 10^4 E0771 cells, mock or constitutively secreting IFN- β, IFN-λ, or IFN- β -IFN-λ, or IFN- β and IFN-λ in a 50:50 ratio were injected orthotopically into the mammary fat pad of female C57BL/6 mice. Tumor growth was monitored every 3-5 days for 4 weeks, and tumor volumes are shown as relative mean (**d, f**) or individual (**e, g**) tumor volumes compared to the mean volume of mock-transfected tumors measured at the end point (day 29). **(h)** Mice injected with E0771 cells expressing IFN- β and IFN-λ in 50:50 showed ascites, whereas the mice injected with the IFN- β -IFN-λ fusion did not show this phenotype. **(i)** Tumors expressing the IFN- β -IFN-λ fusion protein, and livers from these mice, show reduced anemia compared to the tumors expressing IFN- β and IFN-λ in 50:50.

Gas6(Gla+EGF)-IFN-β-IFN-λ proteins display both IFN activity and PS binding characteristics

Next, to target IFNs to tissues with chronically externalized PS, a strategy was designed to transform the tumor from an immuno-suppressive (cold) to a pro-inflammatory (hot) microenvironment. Single IFNs and the IFN-β-IFN-λ fusion protein were further fused to the Gla domain or the Gla and EGF-like domains of Gas6 (a PS-binding TAM receptor ligand), creating bi-functional Gas6-IFN fusion proteins

doi.org/10.32388/TMAXT9

(**Fig. 3.a.**). Having shown that recombinant type I and type III IFN fusion molecules can be stably generated and retain the intrinsic biological activities of both IFN moieties, we fused IFNs, either alone or in tandem, to the Gla domain or Gla plus 4 tandem EGF-like domains of Gas6, hence endowing these proteins with the ability to bind externalized PS. In other iterations of these fusion proteins, phosphorylation labeling sites, GFP fusions, and Fc fusions were introduced to facilitate labeling and in vivo localization (**Supplementary table 1**). PS has been well studied as a global immunosuppressive signal[26] and targeting PS by utilizing Gas6-IFN fusion molecules is expected to target IFNs to a PS-positive environment and convert global immunosuppressive signals into IFN-promoted immunostimulatory signals (**Fig.3.a.**).

To assess whether Gas6-IFNs also retain PS-binding capabilities, we first prepared fusion proteins by culturing HEK293 cells in the presence of vitamin K or Warfarin (the latter blocks γ-carboxylation of the Gas6 Gla domain) (**Fig. 3.b.**), as shown by immunoblotting with an anti-Gla antibody. As previous studies have shown that γ-carboxylation is required for PS binding[28][29], this biochemical approach permits the development of fusion proteins with and without the ability to bind PS-positive cells, as shown in the solid-phase ELISA using affinity-purified recombinant His-tagged proteins (**Fig. 3.c.**). Preferential PS binding was also observed when recombinant proteins were incubated with CDC50A^{ED29} cells, a mutant cell line that fails to internalize PS and that shows constitutively externalized PS on live cells (**Fig. 3.d.**) [30][31]. Following calcium ionophore treatment, cells were incubated with fusion molecules for 5 min, and their binding on the surface of normal and stressed cells was detected with His Ab using flow cytometry. Similar to the PS ELISA, only γ-carboxylated Gas6-IFN-β-IFN-λ was able to bind the externalized PS on the surface of stressed H1299 cells in a pattern similar to Annexin-V **(Supplementary figure 3.f.**), which was used as a positive control for PS binding in flow cytometry. These data demonstrate that under conditions of cell stress, mimicked here by calcium ionophore, Gas6-IFNs bind to cells with externalized PS and therefore are predicted to "home to" a stressed environment with constitutively externalized PS, such as a tumor microenvironment. Additionally, in order to assess if the replacement of the LG domains of Gas6 with IFN domains in the Gas6(Gla+EGF)-IFN-β-IFN-λ fusion proteins has an effect on the efferocytosis capability of these modified Gas6 ligands, we treated BMDMs with apoptotic Jurkat cells in the presence of the fusion proteins. The IFN fusion proteins were seen to significantly reduce efferocytosis of apoptotic cells by BMDMs, indicating a potential anti-tumorigenic effect (**Supplementary Fig.3.g.)**

To better substantiate this latter idea, we employed a CHO IFN-λ reporter cell line, which expresses a modified IFN-λ receptor complex composed of the intact IL-10R2 and the chimeric IFN-λR1/IFN-γR1 chain where the IFN-λR1 extracellular domain is fused to the intracellular IFN-γR1 domain. Accordingly, in the presence of IFN-λ2, the reporter receptor will dimerize and activate IFN-γR1-specific signaling, leading to phosphorylation of STAT1 as a readout (**Fig. 3 e,f**). As indicated by the detection of pSTAT1, these reporter cells respond to fusion proteins containing IFN-λ, including IFN-β-IFN-λ and Gas6-IFN-β-IFN-λ fusion proteins prepared in the presence of vitamin K or Warfarin, when treated with IFNs with or without apoptotic cells for 30 minutes. To reiterate PS binding function, fusion proteins were incubated with CDC50A^{ED29} cells (**Fig.3.e.**) or apoptotic cells (**Fig.3.f.**) for 5 mins, followed by centrifugation, and the cell pellet was washed twice with DMEM medium to remove unbound proteins. Subsequently, the cell pellet containing CDC50A^{ED29} cells or apoptotic cells was used to induce STAT1 phosphorylation in the IFN-λ reporter cells. As shown by immunoblot analysis, pSTAT1 was detected only with γ-carboxylated Gas6-IFN-β-IFN-λ protein bound to CDC50A^{ED29} cells (**Fig. 3.e**) or apoptotic cells **(Fig. 3.f.)**. A priori, these data indicate that γ-carboxylated Gas6-IFN fusion proteins can simultaneously bind PS and at the same time activate IFN receptors.

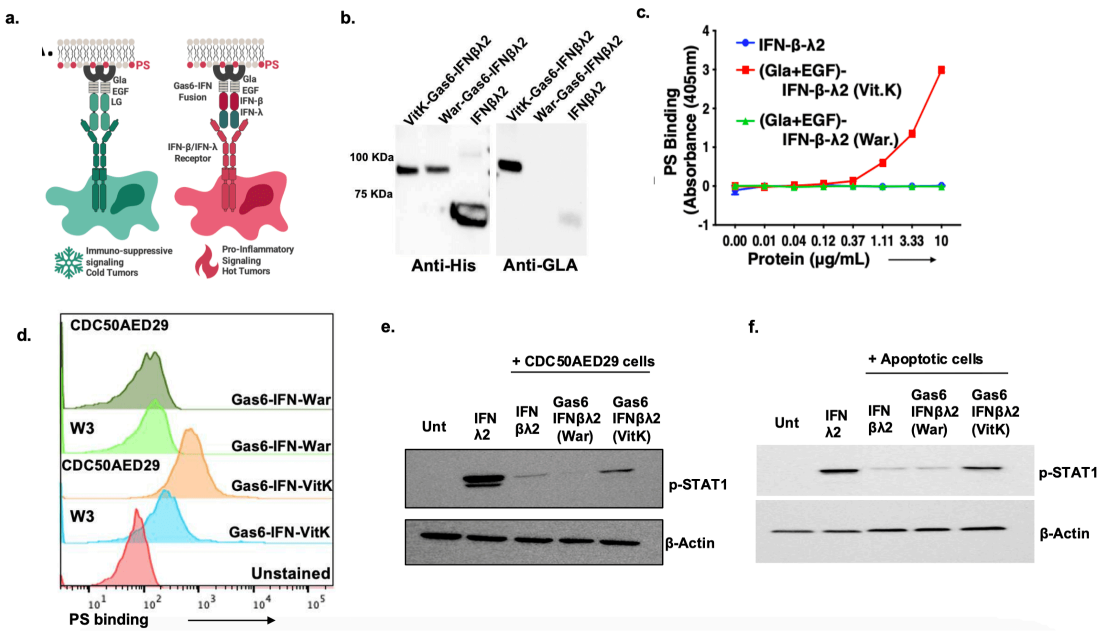


Figure 3. Gas6-IFN-βλ2 (Vit-K) proteins display both IFN activity and PS binding characteristics. (a) Schematic showing the rationale for developing Gas6(Gla+EGF)-IFN-β-IFN-λ fusion proteins; Gla and EGF domains of Gas6 are required for PS binding, whereas the LG domain activates immunosuppressive TAM receptor signaling. Truncating the Gas6 and replacing the LG domains with immunomodulatory IFN fusions will convert immunosuppressive signaling to pro-inflammatory signaling. **(b)** γ-carboxylated (PS binding) and non γ -carboxylated (non PS binding) variants of Gas6(Gla+EGF)-IFN-β-IFN-λ were produced by supplementing transfected HEK293T cell media with vitamin K or Warfarin, respectively, during protein production. **(c)** PS ELISA confirms that γ-carboxylated Gas6(Gla+EGF)-IFN-β-IFN-λ binds to PS, whereas IFN-β-IFN-λ does not. **(d)** This is further confirmed by using CDC50A^{ED29} cells, a mouse lymphoma cell line (W3) that harbors a mutation in CDC50, leading to the loss of PS-flippase function and constitutive externalization of PS on live cells. Gas6(Gla+EGF)-IFN-β-IFN-λ (VitK) binds to only CDC50A^{ED29} (PS^{+}) cells, whereas Gas6(Gla+EGF)-IFN-β-IFN-λ (War) does not bind to either. **(e)** CHO IFN-λ reporter cells were treated with IFN-β-IFN-λ, Gas6(Gla+EGF)-IFN-β-IFN-λ (VitK), and Gas6(Gla+EGF)-IFN-β-IFN-λ (War) with CDC50A^{ED29} cells **(f)** or apoptotic cells for 15 min, washed and centrifuged to remove unbound protein, and incubated with reporter cells for 30 min. Immunoblot of pSTAT1 is used as a readout of IFN-λR activation in the reporter cells.

Gas6-IFN-βλ2 (Vit-K) displays a unique clustered pattern of binding on PS^{+} cells

To explore the effects of the addition of the Gas6 domain to the IFNβ-IFN-λ fusion proteins, we developed several iterations of this protein, with either the Gla domain only (Gas6 (Gla)-IFN-β-IFN-λ, Gas6 (Gla)-

doi.org/10.32388/TMAXT9

IFN-β, Gas6 (Gla)-IFN-λ) or Gas6 containing both the Gla and EGF domains (Gas6 (Gla+EGF)-IFN-λ, Gas6(Gla+EGF)-IFN-β, and Gas6 (Gla+EGF)-IFN-β-IFN-λ) (**Fig.4.a.)**. When these proteins were expressed in HEK293 cells (cultured in the presence of Vitamin K to allow γ-carboxylation of the Gas6 Gla domain), both Gas6(Gla)-IFNs and Gas6 (Gla+EGF)-IFNs were produced, as shown by immunoblotting with anti-His (**Fig.4.b.)** and were effectively γ-carboxylated as evident by immunoblotting with mAb against a γ-carboxylated Gla domain (**Fig.4.c**.). Interestingly, proteins that contained the 4 tandem EGF-like domains appeared as both monomers and dimers, suggesting that the EGF-like domains control a level of oligomerization (**Figs. 4.b. and 4.c)**. This EGF-mediated clustering of PS-binding Gla proteins can also be observed by amplification of PS receptor (Mertk) signaling in the presence of a PS source such as apoptotic cells or PS liposomes (**Fig.4.d.)**. When Mertk-***γ***R1 reporter cells (Mertk-R1 reporter construct contains extracellular and transmembrane regions of Mertk and the intracellular kinase domain of IFN receptor) are treated with full-length Gas6 (Gla+EGF+LG) (**Fig.3.a**.), Mertk is hyperactivated in the presence of PS, provided by apoptotic cells or PS liposomes, perhaps by the clustering of the Gas6 ligands (**Fig.4.d**). Having shown that Gas6-IFN--2 (VitK) preferentially binds to PS on W3-Ildm CDC50A^{ED29} cells, we explored the pattern of surface binding on these cells. For this, we used imaging flow cytometry or AMNIS. Cells were prepared as they were for flow cytometry, and images were collected at 60X magnification on ImageStream AMNIS. After gating on the singlet cell population, dead cells were gated out using 7AAD staining (**Supplementary figures 3.a-3.c.)**. Interestingly, Gas6-IFN--2 (VitK)-His-PE showed a unique pattern of binding wherein the fluorescence appeared to be clustered or polarized on the cell surface (**Fig.4.e.**), whereas a more diffuse binding pattern was observed in the IFN--2-His-PE samples (**Fig.4.f**), perhaps indicating a pattern of binding to the IFN receptors on these cells. Annexin V-PE showed a uniform binding pattern compared to the Gas6-IFN--2 (VitK)-His-PE **(Fig.4.g.)**. Further analysis showed that the “diffuse staining” population was enriched in the cells treated with IFN--2-His-PE (**Fig.4.h.)**, whereas the “polarized staining” population was enriched in the cells treated with Gas6-IFN--2 (VitK)-His-PE (**Fig.4.i.**). Gas6-IFN--2 (War)-His-PE did not have many positive cells to analyze, since they did not show preferential PS binding (Supplementary **Fig.3.e**.) This unique pattern of polarized staining in the PS-dependent binding of Gas6-IFN--2 (VitK)-His-PE supports the idea that Gla+EGF domains are driving the clustering of the PS-targeting molecules, as well as to other Gas6-IFN--2 (VitK) fusion proteins, by engaging certain inter-molecular bonds.

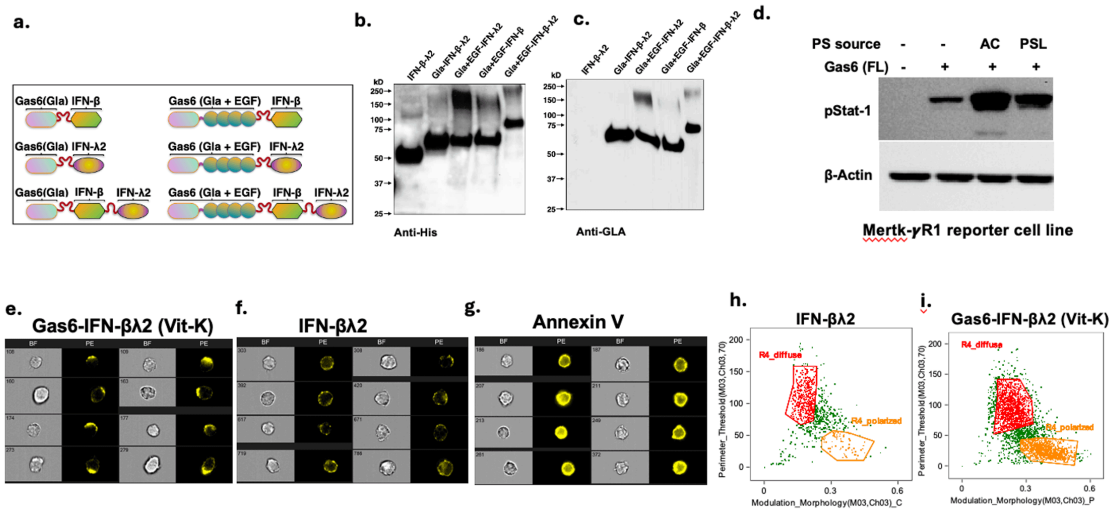


Figure 4. Gas6-IFN-βλ2 (Vit-K) displays a unique clustered pattern of binding on PS$^+$ cells a) Schematic diagram showing the different Gas6-IFN fusion proteins developed with just the Gla domain or the Gla and EGF domains of Gas6 with IFN-β, IFN-λ, or IFN-β-IFN-λ, i.e., Gas6(Gla)-IFN-β, Gas6(Gla)-IFN-λ, Gas6(Gla)-IFN-β-IFN-λ, and Gas6(Gla+EGF)-IFN-β, Gas6(Gla+EGF)-IFN-λ, Gas6(Gla+EGF)-IFN-β-IFN-λ. **(b)** Immunoblot showing secretion of each protein at their expected molecular weight in the cell supernatant when probed using an anti-His antibody and confirming the γ- carboxylation on the Gla domain using an anti-Gla antibody **(c).(d)** Activation of the Mertk--R1 reporter cell line using Gas6 and PS shows that the addition of PS in the form of apoptotic cells or PS liposomes shows hyperactivation of Mertk. Imaging flow cytometry shows a distinct pattern of fusion protein binding to CDC50A^{ED29} (PS$^+$) cells. **(e)** Gas6-IFN-β-IFN-λ (VitK) shows a clustered pattern of binding, whereas **(f)** IFN-β-IFN-λ2 shows a more diffuse pattern of staining. **(g)** Annexin-V-PE binds uniformly compared to Gas6-IFN-β-IFN-λ (VitK) **(h)** Quantification of the diffuse vs. the clustering pattern shows a more diffuse pattern with IFN-β-IFN-λ2 versus a clustered pattern with Gas6-IFN-β-IFN-λ (VitK).

IFN-β-IFN-λ and Gas6-IFN-β-IFN-λ fusion proteins show anti-tumor efficacy in E0771 and B16-F10 tumor models

In order to test the anti-tumor efficacies in vivo, the E0771 or B16 tumor cells were stably transfected with plasmids containing the above-mentioned constructs, which were then actively secreted by the clonally-derived tumor cells. The E0771 and B16 cells expressing IFN-β-IFN-λ or the Gas6(Gla+EGF)-IFN-β-IFN-λ were themselves protected from virus infection (**Supplementary figure 1.c.).** Analogous to IFN-β and IFN-λ above, all fusion proteins displayed antiviral protection on respective cell lines that are sensitive to

only mouse type I IFNs (LA4 cells) (**Supplementary figure 2.a.**) or mouse type III IFNs (ARPE19 cells) (**Supplementary figure 2.b**.). This demonstrates that fusion of monomeric or dimeric IFNs to Gas6 Gla or Gla-EGF domains retains their intrinsic biological activities of IFNs as Gas6-IFN fusion chimeric proteins.

Interestingly, while Gas6(Gla)-IFN-β-IFN-λ, Gas6(Gla+EGF)-IFN-λ, and Gas6(Gla+EGF)-IFN-β all showed partial reduction in tumor volume, the Gas6(Gla+EGF)-IFN-β-IFN-λ showed a more robust effect and completely blocked tumor growth. This suggests that the IFN-β-IFN-λ duet is the more optimal combination of IFNs, but also that the EGF-like domains of Gas6 likely participate in signaling, possibly by stabilizing the protein or inducing a form of oligomerization (**Fig. 5.a, 5.b.**). This is further supported by the observations shown in **Fig. 5.c, 5.d** that a 50:50 mixture of cells expressing either Gas6(Gla+EGF)-IFN-β or Gas6(Gla+EGF)-IFN-λ did not phenocopy the tumor growth profile of cells expressing the Gas6(Gla+EGF)-IFN-β-IFN-λ fusion protein.

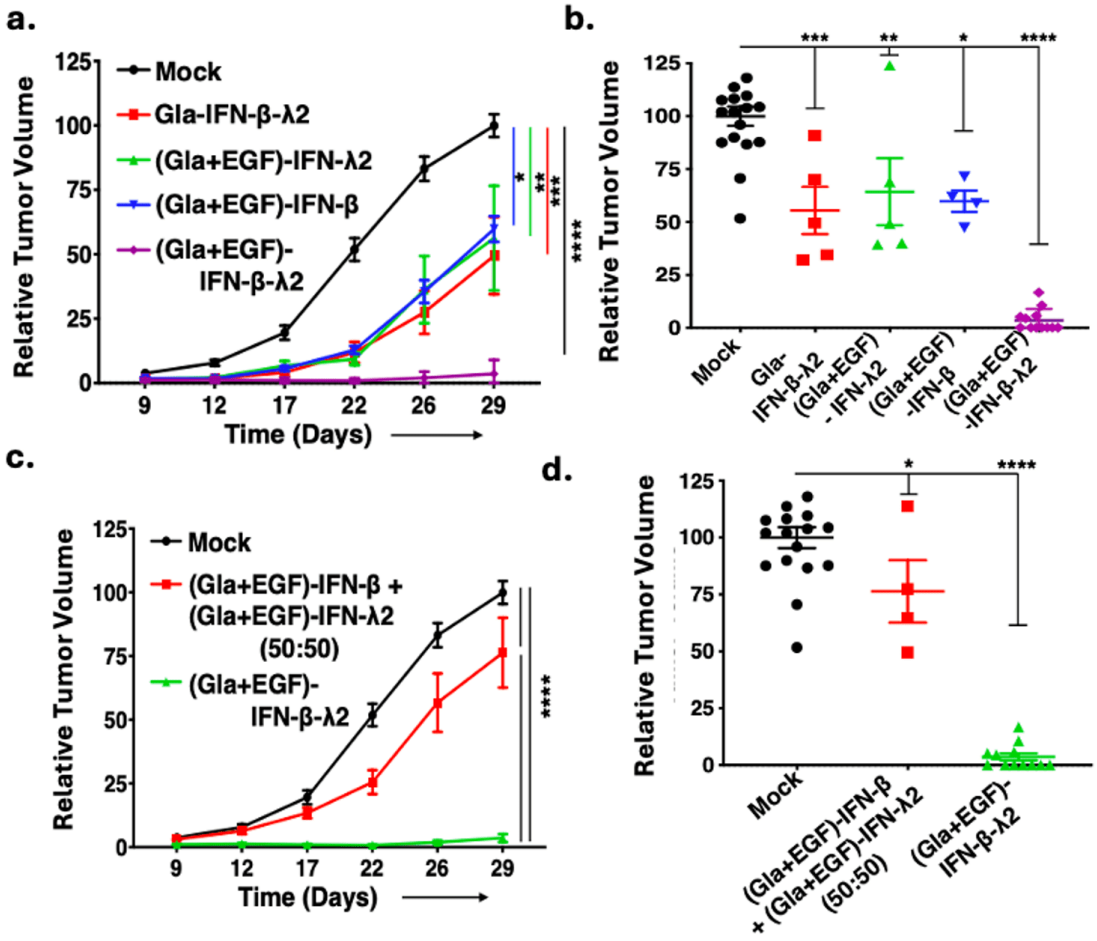


Figure 5. IFN-β-IFN-λ and Gas6-IFN-β-IFN-λ fusion proteins show anti-tumor efficacy in E0771 and B16-F10 tumor models. *In vivo* tumor growth curves of E0771 and B16-F10 tumor models. 5 X 10^4 E0771 cells, mock transfected, or constitutively secreting either Gas6(Gla)-IFN-β-IFN-λ, Gas6(Gla+EGF)-IFN-λ2, Gas6(Gla+EGF)-IFN-β, or Gas6(Gla+EGF)-IFN-β-IFN-λ, were injected orthotopically into the mammary fat pad of C57BL/6 mice, and tumor growth was determined by tumor volume measurements every 3-5 days for a period of 4 weeks. To compare the anti-tumor effects of Gas6-IFN-β-IFN-λ fusion protein to the effects of Gas6-IFN-β and Gas6-IFN-λ (single IFN proteins) given in combination, C57BL/6 mice were implanted with 5 X 10^4, E0771 cells producing Gas6(Gla+EGF)-IFN-β-IFN-λ cells or a 50:50 mixture of E0771 cells producing Gas6(Gla+EGF)-IFN-β and E0771 cells producing Gas6(Gla+EGF)-IFN-λ (total number of implanted cells 5 X 10^4). The Gla+EGF domains and the fusion of IFNs β and λ have an additive effect, as shown by the reduction in (a) tumor volume by days and (b) tumor volume at the end point. Similarly, the Gas6(Gla+EGF)-IFN-β-IFN-λ fusion protein was much more potent in inhibiting tumor growth than the 50:50 combination of single IFNs, as shown by relative tumor volume at various time points and at the end point **(c,d).**

doi.org/10.32388/TMAXT9

To expand these observations to a second tumor model, we compared IFN-β-IFN-λ and Gas6 (Gla+EGF)-IFN-β-IFN-λ side-by-side in both the E0771 orthotopic model (**Fig. 6.a.,b.**) and the B16-F10 flank model (**Fig. 6.c.,d.**), and showed that Gas6(Gla+EGF)-IFN-β-IFN-λ performed equally in terms of tumor growth suppression as IFN-β-IFN-λ did, again indicating that the fusion of the PS-binding Gla-EGF domains of Gas6 did not interfere with the biological function of the IFN-β-IFN-λ duet as a trimeric protein (**Fig. 6.a. 6.-d.**).

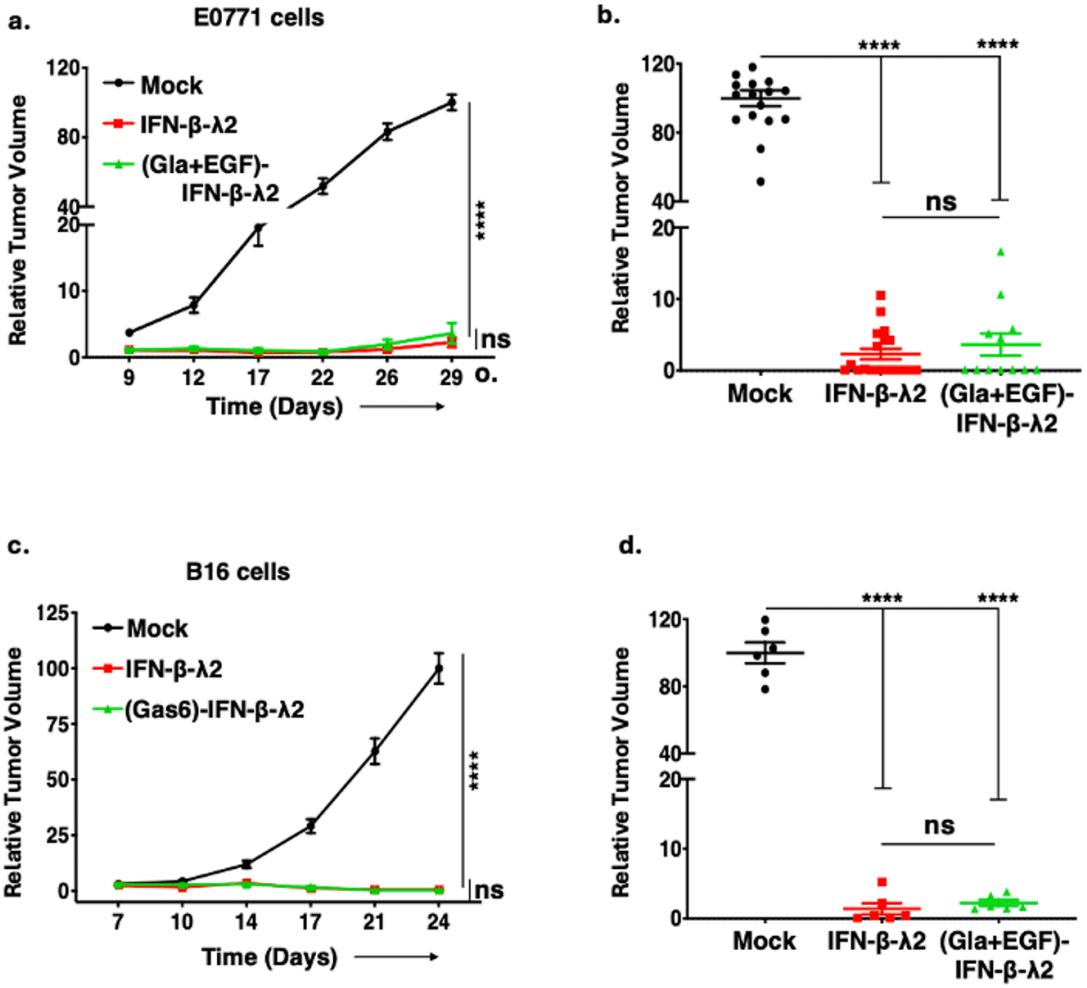


Figure 6. Addition of the Gla and EGF domains does not interfere with anti-tumor activity. To compare the effect of PS targeting on the anti-tumor potency of the IFN-β-IFN-λ fusion molecule, Gas6(Gla+EGF)-IFN-β-IFN-λ and IFN-β-IFN-λ were compared head to head in E0771 **(a, b)** and B16-F10 models **(c, d)**. 5 X 10^4 E0771 or 5 X 10^4 B16 cells, mock-transfected or constitutively secreting either IFN-b-IFN-λ or Gas6(Gla+EGF)-IFN-β-IFN-λ, were injected either orthotopically into the mammary fat pad of female C57BL/6 mice for the E0771 model or into the right flank of C57BL/6 mice for the B16-F10 model.

doi.org/10.32388/TMAXT9

IFN-β-IFN-λ and Gas6-IFN-β-IFN-λ fusion molecules modulate host immune response to exert anti-tumor activity

To investigate the extrinsic role of the tumor microenvironment in the above-mentioned anti-tumor responses, we utilized type I, type III, or type I and type III double IFN receptor knockout (KO) mice on a C57BL/6 background in E0771 and B16-F10 tumor models (**Fig. 7.a**). As shown in **Fig. 7.b.** (E0771) and **Fig. 7.c.** (B16-F10), when cells expressing IFN-β-IFN-λ or Gas6-IFN-β-IFN-λ were transplanted into IFNAR1 KO mice, tumor growth was partially reduced compared to mock-transfected cells. However, compared to tumor growth in the WT C57BL/6 mice, tumors grew substantially better in the IFNAR1 KO, suggesting that type I IFN receptors on tumor-infiltrating immune cells provide a degree of tumor immune surveillance and anti-tumor immunity. In contrast, when IFN-β-IFN-λ or Gas6-IFN-β-IFN-λ expressing tumor cells were transplanted into IFNLR1 KO mice, there was little observable anti-tumor protection (**Fig. 7.d, 7.e**). Similarly, when IFN-β-IFN-λ or Gas6-IFN-β-IFN-λ expressing cells were transplanted into IFNAR1/IFNLR1 double KO mice, the effects of IFNs on tumor growth kinetics were similar to the effects observed in the IFNAR1 single KO mice (**Fig. 7.f, 7.g**). This suggests that type I and type III IFNs act distinctly (likely on different cell types in the TME) and that IFN-β-IFN-λ fusion proteins, as predicted in their design, act on both immune cells (type I IFNs) and on the tumor cells (type III IFNs, see also **Fig. 7.c.**). Consistent with this idea, when IFN-β-IFN-λ or Gas6-IFN-β-IFN-λ expressing tumor cells were transplanted into NOD/SCID mice (E0771 were used in these experiments), tumor growth was only partially suppressed (**Fig.7.h.)** However, when the IFN-β-IFN-λ or Gas6-IFN-β-IFN- λ expressing E0771 cells were injected into Rag1 KO mice, which are deficient in mature T and B cells, all the tumors grew at a similar rate (**Fig.7.i**), suggesting that these fusion proteins exert their anti-tumor effects through the adaptive immune system. Collectively, these data suggest that type I and type III fusion proteins are likely to act to both increase the immunogenicity of tumor cells as well as stimulate immune cells in the tumor microenvironment.

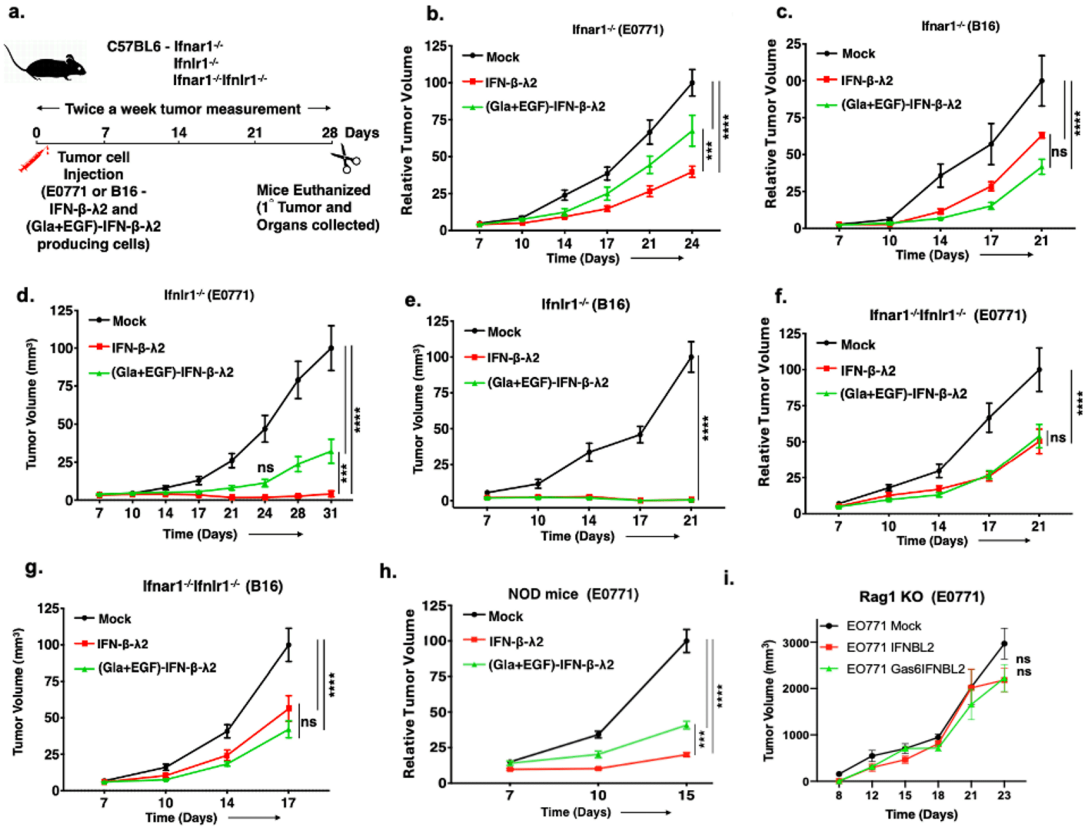


Figure 7. IFN-β-IFN-λ and Gas6-IFN-β-IFN-λ fusion molecules modulate host immune response to exert anti-tumor activity. (a) The graphical outline showing the experimental outline of the E0771 and B16-F10 tumor model in type I, type III, or type I and type III double IFN receptor KO mice on a C57BL/6 background is schematically illustrated. **b-c.** E0771**(b)** and B16-F10 **(c)** mock or constitutively IFN-β-IFN-λ or Gas6-IFN-β-IFN-λ secreting tumor cells were injected into type I IFN receptor (IFNAR1) KO mice, and tumor growth was analyzed. **d-e.** Anti-tumor effects of IFN-β-IFN-λ or Gas6-IFN-β-IFN-λ fusion molecules were also evaluated in type III IFN receptor (IFNLR1) KO mice by monitoring tumor growth dynamics in KO mice injected with mock or IFN fusion molecule-secreting E0771 **(d)** and B16-F10 **(e)** tumor cells. **f-g.** Partial inhibition of tumor growth was also observed when E0771 **(f)** and B16-F10 **(g)** mock or constitutively IFN-β-IFN-λ or Gas6-IFN-β-IFN-λ secreting tumor cells were injected into type I and type III IFN receptor double KO mice **(h).** Mock or constitutively IFN-β-IFN-λ or Gas6-IFN-β-IFN-λ secreting E0771 cells were injected into NOD mice, and tumor growth was analyzed. **(i)** Mock or constitutively IFN-β-IFN-λ or Gas6-IFN-β-IFN-λ secreting E0771 cells were injected into RAG1 KO mice, and tumor growth was analyzed.

doi.org/10.32388/TMAXT9

IFN-β-IFN-λ and Gas6-IFN-β-IFN-λ fusion molecules have direct anti-tumor effects on tumor cells

To explore cell-intrinsic versus cell-extrinsic functions of IFN-β-IFN-λ and Gas6(Gla+EGF)-IFN-β-IFN-λ (subsequently designated as Gas6-IFN-β-IFN-λ) fusion proteins in the E0771 and B16-F10 models of tumor growth, we assessed the induction of cell surface MHC class I protein expression. Bulk RNA sequencing of primary murine lung epithelial (MLE) cells treated with Gas6(Gla+EGF)-IFN-β-IFN-λ VitK for 7 or 24 hours showed differential regulation of early and late induced genes compared to untreated **(Fig. 8.a.)**. Quality control was done by PCA, which showed that replicates cluster together and that the Gas6(Gla+EGF)-IFN-β-IFN-λ VitK-treated samples differ significantly from untreated samples **(Supplementary Fig. 1.e.).** Focusing on genes upregulated at the early time point of 7 hours after treatment, MHC I protein complex and transporter associated antigen processing proteins, Tap1 and Tap2 (**Fig.8.b**.) are seen to be upregulated. Classical ISGs (in green) and PD-L1 (CD274 in red) are also shown to be upregulated (**Fig.8.b**.). Gene ontology enrichment analysis for cellular components identified MHC I protein complexes as most significantly upregulated **(Fig.8.c.)**, whereas regulation of cytokine responses and pathogen response pathways were the most enriched biological processes **(Fig.8.d.)**. While neither protein had notable effects on cell growth or apoptosis (data not shown), both proteins strongly upregulated levels of MHC class I protein and PD-L1 expression on the surface of E0771 cells (**Fig. 8.e.,g.**) and B16-F10 cells (**Fig. 8.f.,h,**), predicting enhanced immunogenicity of the modified tumor cells *in vivo*. Consistent with this idea and to analyze STAT1 phosphorylation as a signature IFN response, we extracted steady-state lysates, and as shown in (**Supplementary Fig. 1.f.**), in both E0771 and B16-F10 cells constitutively producing IFN-β-IFN-λ or Gas6-IFN-β-IFN-λ fusion molecules, STAT1 phosphorylation was robustly stimulated as compared to mock cells. Taken together, these data support the proof of concept for the utility of PS-targeting IFNs, potentially in combination with checkpoint inhibitors such as anti-PD1.

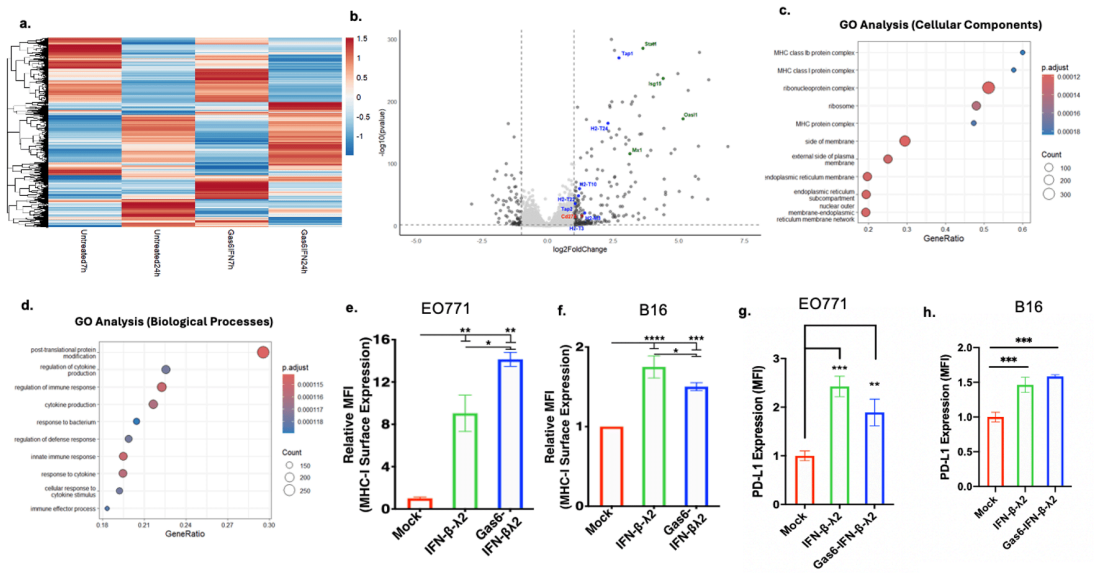


Figure 8. IFN-β-IFN-λ and Gas6-IFN-β-IFN-λ fusion molecules have direct anti-tumor effects on tumor cells: (a) RNA sequencing data show differentially expressed genes upon treatment of MLE cells with Gas6-IFN-β-IFN-λ (VitK) for 7 or 24 hours. **(b)** MHC I, Tap proteins, PD-L1, and classical ISGs are upregulated upon IFN treatment. **(c)** Gene Ontology enrichment revealed that MHC class I protein complexes are upregulated in cells treated with Gas6-IFN-β-IFN-λ (VitK) for 7 hours, and **(d)** biological processes related to pathogen response and cytokine production are also upregulated. E0771 and B16-F10 cells mock-transfected or constitutively secreting either IFN-β-IFN-λ or Gas6-IFN-β-IFN-λ were analyzed for cell surface expression of MHC class I (H-2Kd/H-2Dd) protein and PD-L1 by flow cytometry. The data shown are representative of 3 independent experiments (**e-h**) .The quantification of relative MFI is shown for MHC-I and PD-L1, respectively (**e,g**) for E0771 and (**f,h**) for B16-F10 cells.

Discussion

The importance of membrane asymmetry and the redistribution of PS to the outer leaflet of the plasma membrane has gained much interest in the field of immune-oncology in recent years. Unlike PS externalization on stochastic apoptotic cells that are efficiently cleared by macrophage efferocytosis to maintain homeostasis and tolerance, apoptosis in tumors is chronic and sustained, and many solid tumors exist with high apoptotic indexes (tumors have been called wounds that never heal)[23][12]. Similarly, unlike the rapid and reversible externalization of PS on activated immune cells and in the tumor stroma, PS externalization on viable cells in the tumor microenvironment is also chronic and

doi.org/10.32388/TMAXT9

sustained, leading to the robust activation of inhibitory PS receptors in the tumor microenvironment, as well as exhaustion and anergy of immune cells[60]. Such complex sustained PS externalization in the tumor microenvironments is a pathophysiological mechanism that contributes to tumor immune escape, as recent studies show that activation of PS flippases such as TMEM30A can recapitulate immune dysfunction and evasion of host immunity, while blockage of PS externalization improves host immunity[61]. While previous attempts to block PS in the tumor microenvironment using PS-targeting mAbs and PS binding modalities have shown promising results, few, if any, of these approaches have linked an immunogenic payload to a PS-targeting strategy[62]. Here, we report on a new class of PS-targeting modality that fuses a type I and type III IFN duet to the phosphatidylserine binding domain of Gas6, expected to introduce an immunogenic payload to the tumor micro-environment (Fig.9).

Type I and type III IFNs bind to different receptor complexes, namely type I (IFNAR) and type III (IFNLR) IFN receptors, respectively[63]. While both type I and type III IFN receptors activate a common post-receptor Jak-STAT signaling pathway, recent studies reveal that receptor expression patterns are functionally compartmentalized[59][64]. Here, we demonstrate that recombinant fusion proteins that combine type I (IFN-β) and type III (IFN-λ) enhance both antiviral and anti-tumor activity compared to monomeric IFN species, and that this activity is retained when IFN-β-IFN-λ is further linked to the PS-binding domain of Gas6. As such, our approaches highlight the functional co-operativity of type I and type III IFNs as therapeutic entities, and that this synergy can be harnessed using single-chain chimeric fusion proteins. While previous studies have shown that co-administration of IFN-α and IFN-λ provides a synergistic antitumor effect in the mouse model of hepatocellular carcinoma[55], likely attributed to distinct patterns of cell type and tissue distribution of the IFN receptors, the present approach permits focal localization of IFNs and potentially reduces the side effects of type I IFNs. Moreover, the finding that IFN-β-IFN-λ retains full activity when fused to a PS-targeting Gla domain posits that such molecules can be used to specifically target areas of high local PS exposure, such as the microenvironments of solid tumors as well as in areas of viral infection. The present study provides a proof-of-concept milestone for the use of functional gain-of-function chimeric type I and type III IFN fusion proteins for potential therapeutic applications.

The idea that type I and type III IFNs will target both immune cells and epithelial cells to improve efficacy is predicted by the differences in tissue distribution of IFNAR and IFNLR. The concept that fusing IFN-β-IFN-λ to the Gla and EGF-like domains of Gas6 is expected to add a level of localized action to IFNs to target specific areas of stressed and diseased cells and exploit a fortuitous vulnerability in cancer and

virology, as noted above[12][24][65]. Two of the better-understood strategies to target PS include recombinant Annexin V proteins[26][66][67] and PS-targeting mAbs generated in the Thorpe laboratory and subsequently developed into preclinical and clinical utilities by Peregerine Pharmaceuticals[27][68][69][70]. In the case of recombinant Annexin V, previous studies have shown that Annexin V, when administered *in vivo*, can improve host anti-tumor immunity, presumably by blocking immunosuppressive signals from PS[13]. Annexin V also renders apoptotic tumor cells immunogenic; the addition of Annexin V to apoptotic tumor cell vaccines increased the percentage of tumor-free mice in syngeneic tumor cure assays[71]. More recently, the administration of Annexin V was shown to significantly enhance immunogenicity and anti-tumor efficacy when administered with chemotherapy and further showed synergy with immune checkpoint inhibitors[67]. Analogous to the biology of Annexin V, PS-targeting mAbs, including Bavituximab and mch1N11, have also shown promising pre-clinical activities, often leading to increased immunogenicity in tumors, increased influx of CD4 and CD8 T cells, and synergy with immune checkpoint inhibitors and radiation therapy[27][14]. In recent years, the repertoire of PS-targeting approaches has gained further traction, including the development of PS-targeting agents as cationic small molecules (QW4869)[72], 2GPI binding F(ab)2 fusion proteins[73] , Annexin fusion proteins (to cystathione gamma-lyase)[74], nanovesicles that target PS (SapC-DOPS)[31][75] , and peptide-peptoid hybrids (PPS1D1)[76]. While such strategies have versatility to modify payloads, most of the current PS-targeting strategies aim to target PS in stressed/diseased tissues; they lack an immunogenic payload. The Gas6-IFN fusions described here not only directly target PS but also divert immunosuppressive signals into immunogenic signals to enhance antiviral and anti-tumor immune responses.

While the present study shows feasibility and proof-of-concept assurance that trimeric fusions, when produced locally in the tumor microenvironment, retain biological activities as active IFNs with PS-targeting capacity, future studies will be required to optimize their *in vivo* delivery and to determine whether they can be injected systemically or intra-tumorally. For PS-targeting mAbs, such as Bavituximab, systemic infusion of mAbs leads to honing and localization in the tumor microenvironment. We also expect that Gas6-IFNs can be applied systemically, since Gas6 has nanomolar affinity toward PS, and the Gla domains of Gas6 have been shown to cluster and/or oligomerize around PS that is constitutively externalized in the tumor microenvironment. In sum, we hypothesize that the targeting of Gas6-IFN-IFN will have an important role in activating host anti-tumor immunity. Indeed, this strategy is in line with emerging concepts that PS in the tumor microenvironment is

immunosuppressive and that type I and type III IFNs have dual compartmentalized models of immune activation. Moreover, since Gas6-IFN-IFN induces MHC class I and PD-L1 on the PS-positive cells, these molecules might prove beneficial via the combined effects of checkpoint therapeutics such as anti-PD1 or anti-PD-L1.

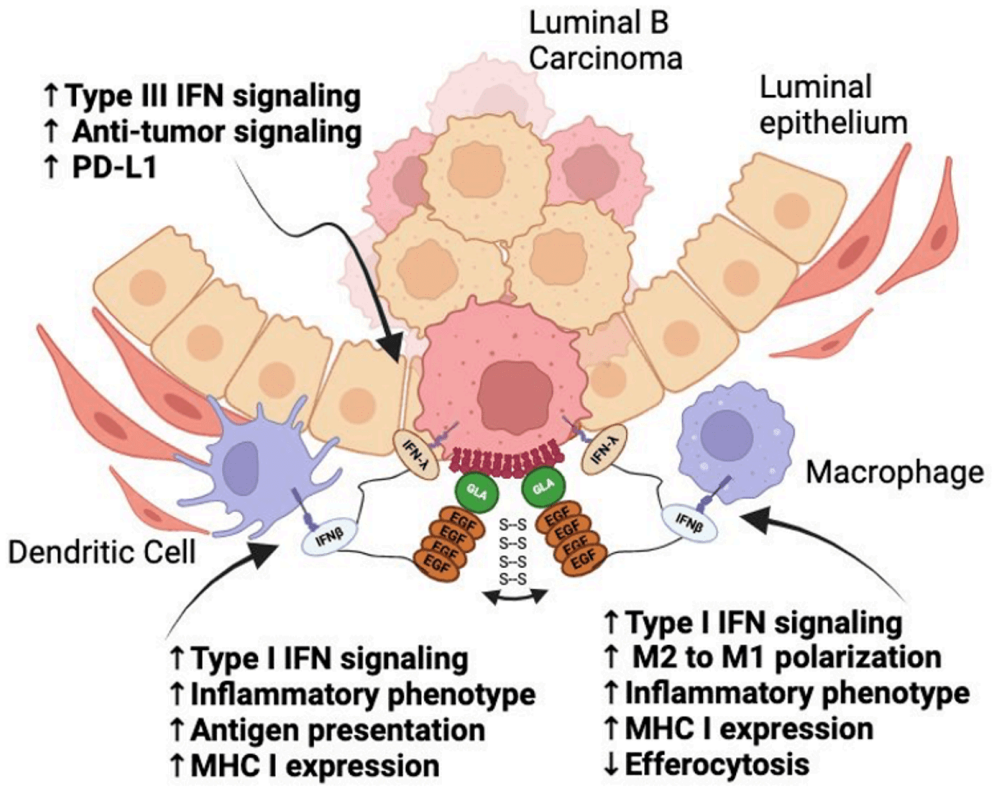
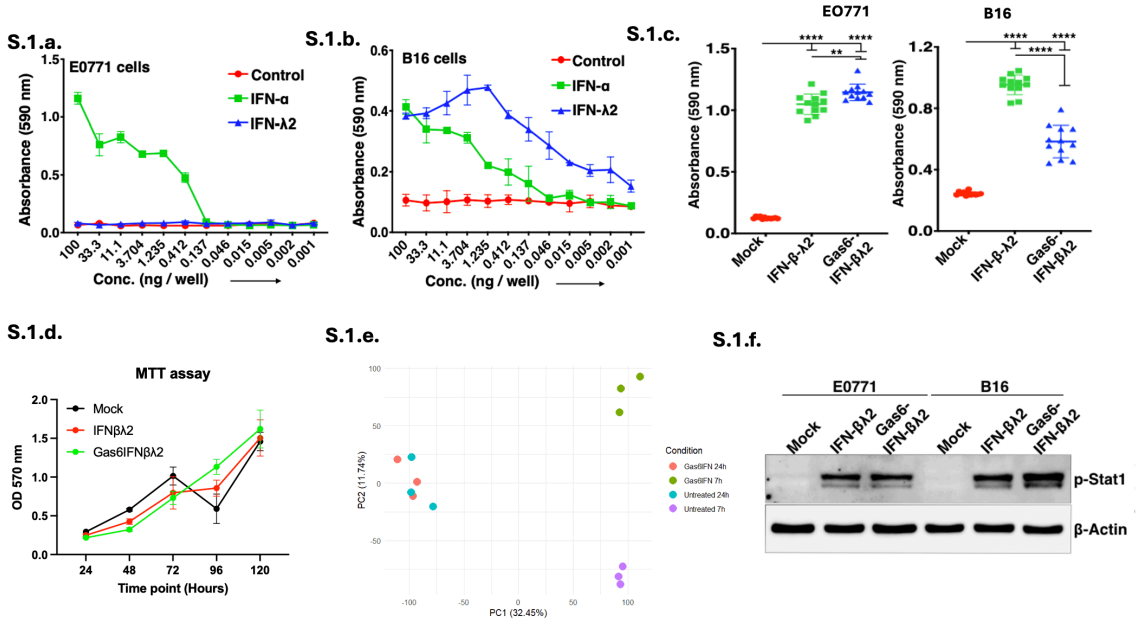


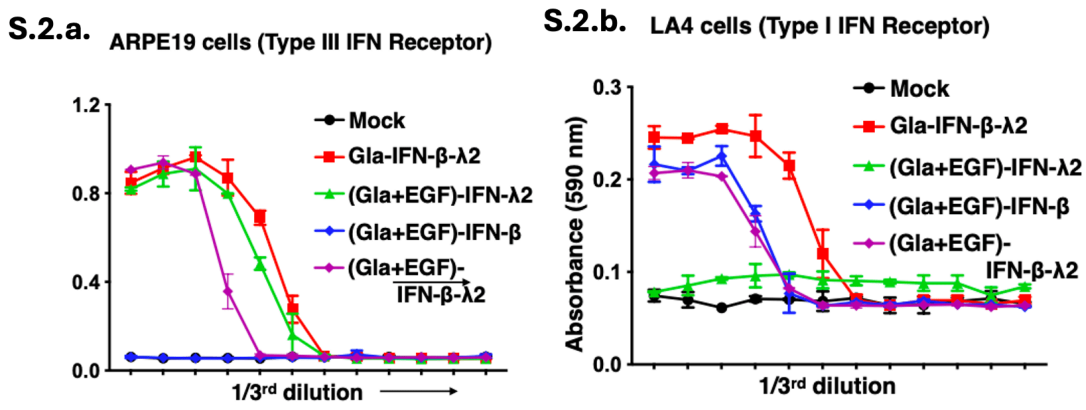
Figure 9. Graphical abstract. Gas6-IFN-β-IFN-λ (VitK) have tri-functional activities, acting on a diverse set of cell types to induce an anti-tumor effect. The Gas6 domain aids in homing to the PS-rich tumor microenvironment, binding to apoptotic or live stressed PS-positive tumor cells. The Gla domain directly binds to PS, whereas the EGF domains help in oligomerization and signal amplification resulting from intermolecular disulphide bonds. The IFN-β domain acts on immune cells such as dendritic cells and macrophages, inducing an interferon response, whereas the IFN-λ domain acts on the tumor epithelial cells, inducing tumor-intrinsic anti-tumor activity.

Supplementary Figures



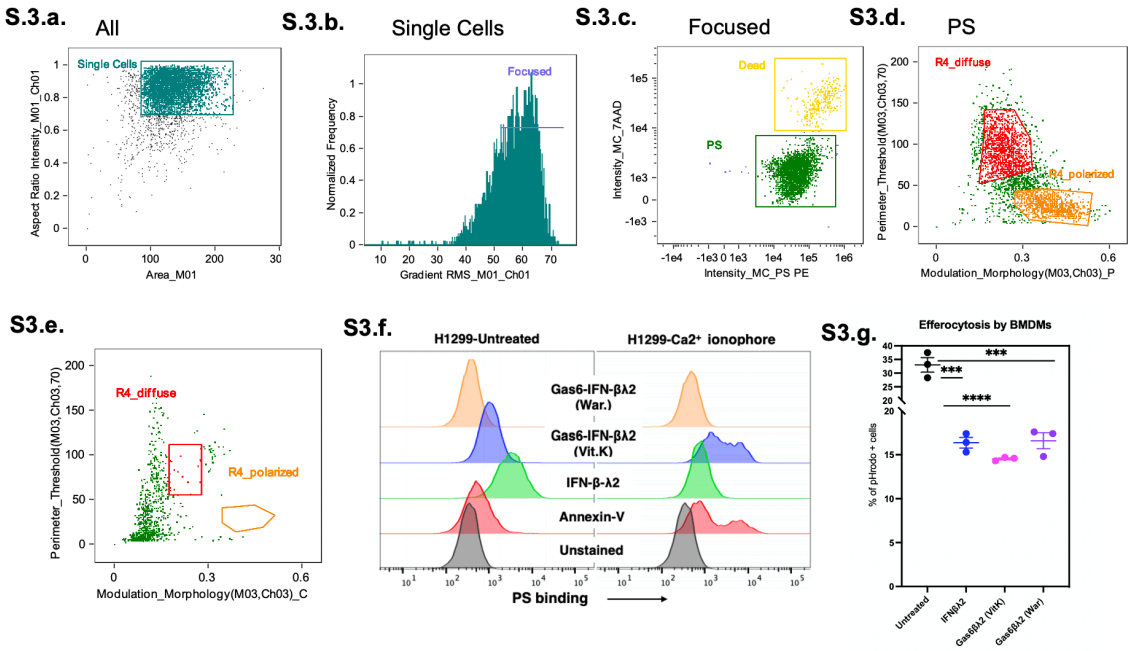
Supplementary Figure 1. Antiviral assay with **(a)** E0771 and **(b)** B16 cells shows that E0771 cells respond only to type I IFNs (IFN-) and B16 cells respond to both type I IFNs (IFN-) and type III IFNs (IFN-). **(c)** Shows protection against antiviral from VSV-GFP using IFN fusion proteins in EO771 and B16 cells, as shown by crystal violet staining. **(d)** MTT assay shows no significant differences in cell viability of E0771 cells producing IFN fusion proteins. **(e)** Principal component analysis of RNA sequencing data from cells treated with Gas6(Gla+EGF)-IFN-λ2(VitK) for 7 or 24 hours shows clustering of samples. **(f)** IFN fusion proteins activate IFN signaling, as seen by upregulation of p-STAT-1 in E0771 and B16 cells.

doi.org/10.32388/TMAXT9



Supplementary Figure 2. Antiviral activities of Gas6(Gla)-IFN-β-IFN-λ, Gas6(Gla+EGF)-IFN-λ2, Gas6(Gla+EGF)-IFN-β, or Gas6(Gla+EGF)-IFN-β-IFN-λ protein-containing HEK293T supernatants are measured in **(a)** LA4 and **(b)** ARPE19 cells.

doi.org/10.32388/TMAXT9



Supplementary Figure 3. Gating scheme for the imaging flow cytometry done in Figure 4. Single cells were gated by area and aspect ratio of the events collected **(a,b).** Live cells were gated (green) by excluding dead cells (yellow) that stained positive for 7AAD **(c)**. The surface staining pattern was quantified by measuring the perimeter staining and the morphology **(d)**. Gas6(Gla+EGF)-IFN-β-IFN-λ (War) did not show binding to CDC50A^{ED29} cells **(e). (f)** H1299 cancer cells were treated with A23187 to induce calcium stress-mediated PS exposure. Only Gas6(Gla+EGF)-IFN-β-IFN-λ (VitK) binds to PS^{+} cells, like Annexin V, which was used as a positive control for binding to externalized PS. IFN fusion proteins blocked efferocytosis of apoptotic cells by bone marrow-derived macrophages **(g).**

doi.org/10.32388/TMAXT9

S.No.	Novel fusion protein	Type –I IFN activity	Type –III IFN activity	PS binding activity (Active Gla)	EGF oligomerization domains	Function
1.		✓	X	X	X	Prophylactic for anti-viral
2.		X	✓	X	X	Prophylactic for anti-viral
3.		✓	✓	X	X	Prophylactic for anti-viral
4.		✓	✓	X	X	Clip and Ph tags for radiolabeling
5.		✓	✓	X	X	GFP for visualizing localization
6.		✓	X	✓	X	Therapeutic for anti-tumor or anti-viral
7.		X	✓	✓	X	Therapeutic for anti-tumor or anti-viral
8.		✓	✓	✓	X	Therapeutic for anti-tumor or anti-viral
9.		✓	X	✓	✓	Therapeutic for anti-tumor or anti-viral
10.		X	✓	✓	✓	Therapeutic for anti-tumor or anti-viral
11.		✓	✓	✓	✓	Therapeutic for anti-tumor or anti-viral (Lead)
12.		✓	✓	✓	✓	Clip and Ph tags for radiolabeling
13.		✓	✓	✓	✓	Fc tag for increasing half life in vivo
14.		✓	✓	✓	✓	GFP for visualizing localization

Supplementary Table 1. Shows the iterations of IFN fusion proteins that can be used for developing pre-clinical models and for therapeutics.

Statements and Declarations

Funding

This work was supported in part by NIH R01 CA260137-01A1 from the National Cancer Institute to RBB and SVK.

Conflicts of interest

SVK and RBB are cofounders of a biotechnology company called Targeron Therapeutics, LLC, that aims to develop PS-targeting IFNs for immune-oncology applications.

Ethics Statement

All animal procedures were conducted in accordance with institutional guidelines and approved by the Rutgers Institutional Animal Care and Use Committee (IACUC), protocol number 201702590. All animal experiments were conducted in accordance with the ARRIVE guidelines.

Authors' contributions

VG and VD contributed equally to the study design, data acquisition, and manuscript preparation. RP, TF, CV, AA, ZW, SS, SB, and DC contributed to data acquisition and analysis. AC provided key resources and support. SVK and RBB supervised the project and contributed equally to its conceptualization and finalization.

Data availability

The datasets generated and/or analyzed during the current study are available from the corresponding author on reasonable request.

Consent to Participate

Not applicable.

Acknowledgements

We thank Dr. Shigekazu Nagata from Osaka University for kindly providing the W3-Ildm CDC50A^{ED29} cells. We thank members of our laboratory for helpful discussions. This work was supported in part by NIH R01 CA260137-01A1 from the National Cancer Institute to RBB and SVK. Biorender was used to create figures.

References

1. ^*Agarwal D, et al. (2025). "Advances in Vaccines, Checkpoint Blockade, and Chimeric Antigen Receptor-Based Cancer Immunotherapeutics." Crit Rev Immunol. **45**(1):65-80.*
2. ^*Sharma P, et al. (2023). "Immune checkpoint therapy-current perspectives and future directions." Cell. **186**(8):1652-1669.*
3. ^*Sharma P, et al. (2021). "The Next Decade of Immune Checkpoint Therapy." Cancer Discov. **11**(4):838-857.*
4. ^*Budczies J, et al. (2024). "Tumour mutational burden: clinical utility, challenges and emerging improvements." Nat Rev Clin Oncol. **21**(10):725-742.*
5. ^*Fares CM, et al. (2019). "Mechanisms of Resistance to Immune Checkpoint Blockade: Why Does Checkpoint Inhibitor Immunotherapy Not Work for All Patients?" Am Soc Clin Oncol Educ Book. **39**:147-164.*

6. ^Labani-Motlagh A, Ashja-Mahdavi M, Loskog A (2020). "The tumor microenvironment: a milieu hinderin g and obstructing antitumor immune responses." Frontiers in immunology. **11**:940.
7. ^Kroemer G, et al. (2022). "Immunogenic cell stress and death." Nat Immunol. **23**(4):487-500.
8. ^Kroemer G, Galluzzi L, Kepp O, Zitvogel L (2013). "Immunogenic Cell Death in Cancer Therapy." Annu Rev I mmunol. **31**:51-72.
9. ^Wu B, et al. (2024). "Cold and hot tumors: from molecular mechanisms to targeted therapy." Signal Transd uct Target Ther. **9**(1):274.
10. ^Ibis B, et al. (2023). "Immune-related adverse effects of checkpoint immunotherapy and implications for t he treatment of patients with cancer and autoimmune diseases." Front Immunol. **14**:1197364.
11. ^Leventis PA, Grinstein S (2010). "The distribution and function of phosphatidylserine in cellular membran es." Annu Rev Biophys. **39**:407-27.
12. a, b, c, d, eBirge RB, et al. (2016). "Phosphatidylserine is a global immunosuppressive signal in efferocytosis, i nfectious disease, and cancer." Cell Death Differ. **23**:962-978.
13. a, bBondanza A, et al. (2004). "Inhibition of phosphatidylserine recognition heightens the immunogenicity of irradiated lymphoma cells in vivo." J Exp Med. **200**(9):1157-65.
14. a, bBudhu S, et al. (2021). "Targeting Phosphatidylserine Enhances the Anti-tumor Response to Tumor-Dire cted Radiation Therapy in a Preclinical Model of Melanoma." Cell Rep. **34**:108620.
15. ^Ran S, Downes A, Thorpe PE (2002). "Increased Exposure of Anionic Phospholipids on the Surface of Tum or Blood Vessels." Cancer Res. **62**:6132-6140.
16. ^Ran S, Thorpe PE (2002). "Phosphatidylserine is a marker of tumor vasculature and a potential target for cancer imaging and therapy." Int J Radiat Oncol Biol Phys. **54**(5):1479-84.
17. a, bSakuragi T, Nagata S (2023). "Regulation of phospholipid distribution in the lipid bilayer by flippases an d scramblases." Nature Reviews Molecular Cell Biology. **24**(8):576-596.
18. ^Nagata S, Sakuragi T, Segawa K (2020). "Flippase and scramblase for phosphatidylserine exposure." Curr Opin Immunol. **62**:31-38.
19. ^Suzuki J, et al. (2013). "Xk-related protein 8 and CED-8 promote phosphatidylserine exposure in apoptotic cells." Science. **341**(6144):403-6.
20. ^Suzuki J, Imanishi E, Nagata S (2016). "Xkr8 phospholipid scrambling complex in apoptotic phosphatidylse rine exposure." Proc Natl Acad Sci. **113**:9509-9514.

21. ^Ryoden Y, Segawa K, Nagata S (2022). "Requirement of Xk and Vps13a for the P2X7-mediated phospholipid scrambling and cell lysis in mouse T cells." Proc Natl Acad Sci U S A. **119**(7).

22. ^Suzuki J, Umeda M, Sims PJ, Nagata S (2010). "Calcium-dependent phospholipid scrambling by TMEM16F." Nature. **468**:834-838.

23. a, bGadiyar V, et al. (2020). "Cell Death in the Tumor Microenvironment: Implications for Cancer Immunotherapy." Cells. **9**(10).

24. a, bKumar S, Calianese D, Birge RB (2017). "Efferocytosis of dying cells differentially modulate immunological outcomes in tumor microenvironment." Immunol Rev. **280**(1):149-164.

25. ^Behuria HG, Dash S, Sahu SK (2022). "Phospholipid scramblases: Role in cancer progression and anticancer therapeutics." Frontiers in Genetics. **13**:875894.

26. a, b, cStach CM, et al. (2000). "Treatment with annexin V increases immunogenicity of apoptotic human T-cells in Balb/c mice." Cell Death Differ. **7**(10):911-5.

27. a, b, cGray MJ, et al. (2016). "Phosphatidylserine-targeting antibodies augment the anti-tumorigenic activity of anti-PD-1 therapy by enhancing immune activation and downregulating pro-oncogenic factors induced by T-cell checkpoint inhibition in murine triple-negative breast cancers." Breast Cancer Res. **18**(1):50.

28. a, bDesai TJ, et al. (2016). "Identification of lipid-phosphatidylserine (PS) as the target of unbiasedly selected cancer specific peptide-peptoid hybrid PPS1." Oncotarget. **7**(21):30678.

29. a, bLee G, et al. (2023). "Development of Apoptotic-Cell-Inspired Antibody–Drug Conjugate for Effective Immune Modulation." International Journal of Molecular Sciences. **24**(22):16036.

30. a, bLi R, et al. (2018). "Targeting Phosphatidylserine with Calcium-Dependent Protein–Drug Conjugates for the Treatment of Cancer." Molecular cancer therapeutics. **17**(1):169-182.

31. a, b, cDavis HW, et al. (2020). "Biotherapy of Brain Tumors with Phosphatidylserine-Targeted Radioiodinated SapC-DOPS Nanovesicles." Cells. **9**(9).

32. ^Pestka S, et al. (1997). "The interferon gamma (IFN-gamma) receptor: a paradigm for the multichain cytokine receptor." Cytokine Growth Factor Rev. **8**(3):189-206.

33. ^Samuel CE (1991). "Antiviral actions of interferon. Interferon-regulated cellular proteins and their surprisingly selective antiviral activities." Virology. **183**(1):1-11.

34. ^Mesev EV, LeDesma RA, Ploss A (2019). "Decoding type I and III interferon signalling during viral infection." Nat Microbiol. **4**(6):914-924.

35. ^Platanias LC (2005). "Mechanisms of type-I- and type-II-interferon-mediated signalling." Nat Rev Immunol. **5**(5):375-86.

36. ^Park A, Iwasaki A (2020). "Type I and Type III Interferons - Induction, Signaling, Evasion, and Application to Combat COVID-19." Cell Host Microbe. **27**(6):870-878.

37. ^Stanifer ML, Pervolaraki K, Boulant S (2019). "Differential Regulation of Type I and Type III Interferon Signaling." Int J Mol Sci. **20**(6).

38. ^Donnelly RP, et al. (2004). "The expanded family of class II cytokines that share the IL-10 receptor-2 (IL-10R2) chain." J Leukoc Biol. **76**(2):314-21.

39. ^Kotenko SV, et al. (2003). "IFN-λambdas mediate antiviral protection through a distinct class II cytokine receptor complex." Nat Immunol. **4**(1):69-77.

40. ^Sheppard P, et al. (2003). "IL-28, IL-29 and their class II cytokine receptor IL-28R." Nat Immunol. **4**(1):63-8.

41. ^Schneider WM, Chevillotte MD, Rice CM (2014). "Interferon-stimulated genes: a complex web of host defenses." Annu Rev Immunol. **32**:513-45.

42. ^Stark GR, Darnell JE Jr (2012). "The JAK-STAT pathway at twenty." Immunity. **36**(4):503-14.

43. ^Lazear HM, Nice TJ, Diamond MS (2015). "Interferon-λ: Immune Functions at Barrier Surfaces and Beyond." Immunity. **43**(1):15-28.

44. ^Lazear HM, Schoggins JW, Diamond MS (2019). "Shared and Distinct Functions of Type I and Type III Interferons." Immunity. **50**(4):907-923.

45. ^Zhou JH, et al. (2018). "Type III Interferons in Viral Infection and Antiviral Immunity." Cell Physiol Biochem. **51**(1):173-185.

46. ^Sistigu A, et al. (2014). "Cancer cell-autonomous contribution of type I interferon signaling to the efficacy of chemotherapy." Nat Med. **20**(11):1301-9.

47. ^Zitvogel L, et al. (2015). "Type I interferons in anticancer immunity." Nat Rev Immunol. **15**(7):405-14.

48. ^Musella M, et al. (2017). "Type-I-interferons in infection and cancer: Unanticipated dynamics with therapeutic implications." Oncoimmunology. **6**(5):e1314424.

49. ^Thyrell L, et al. (2002). "Mechanisms of Interferon-α induced apoptosis in malignant cells." Oncogene. **21**(8):1251-62.

50. ^Corrales L, et al. (2016). "The host STING pathway at the interface of cancer and immunity." J Clin Invest. **126**(7):2404-11.

51. ^Garg AD, Agostinis P (2017). "Cell death and immunity in cancer: From danger signals to mimicry of pathogen defense responses." Immunol Rev. **280**(1):126-148.

52. ^Sprooten J, Agostinis P, Garg AD (2019). "Type I interferons and dendritic cells in cancer immunotherapy." Int Rev Cell Mol Biol. **348**:217-262.

53. ^Lasfar A, et al. (2006). "Characterization of the mouse IFN-λambda ligand-receptor system: IFN-λambdas exhibit antitumor activity against B16 melanoma." Cancer Res. **66**(8):4468-77.

54. ^Li W, et al. (2012). "Type III interferon induces apoptosis in human lung cancer cells." Oncol Rep. **28**(3):1117-25.

55. a, bLasfar A, et al. (2016). "Concerted action of IFN-α and IFN-λambda induces local NK cell immunity and halts cancer growth." Oncotarget. **7**(31):49259-49267.

56. ^Souza-Fonseca-Guimaraes F, et al. (2015). "NK cells require IL-28R for optimal in vivo activity." Proceedings of the National Academy of Sciences. **112**(18):E2376-E2384.

57. ^Burkart C, et al. (2013). "Usp18 deficient mammary epithelial cells create an antitumour environment driven by hypersensitivity to IFN-λ and elevated secretion of Cxcl10." EMBO molecular medicine. **5**(7):1035-1050.

58. ^Segawa K, et al. (2014). "Caspase-mediated cleavage of phospholipid flippase for apoptotic phosphatidylserine exposure." Science. **344**(6188):1164-1168.

59. a, b, cMcElrath C, Espinosa V, Lin JD, Peng J, Sridhar R, Dutta O, et al. (2021). "Critical role of interferons in gastrointestinal injury repair." Nature communications. **12**(1):2624.

60. ^Calianese DC, Birge RB (2020). "Biology of phosphatidylserine (PS): basic physiology and implications in immunology, infectious disease, and cancer." Cell Commun Signal. **18**:41.

61. ^Wang W, et al. (2022). "Mobilizing phospholipids on tumor plasma membrane implicates phosphatidylserine externalization blockade for cancer immunotherapy." Cell reports. **41**(5).

62. ^Huang X, Ye D, Thorpe PE (2011). "Enhancing the potency of a whole-cell breast cancer vaccine in mice with an antibody-IL-2 immunocytokine that targets exposed phosphatidylserine." Vaccine. **29**(29-30):4785-93. doi:10.1016/j.vaccine.2011.04.082. PMID 21557977.

63. ^Levy DE, Marie IJ, Durbin JE (2011). "Induction and function of type I and III interferon in response to viral infection." Curr Opin Virol. **1**(6):476-86.

64. ^Kotenko SV, Durbin JE (2017). "Contribution of type III interferons to antiviral immunity: location, location, location." J Biol Chem. **292**(18):7295-7303.

65. ^Geng K, et al. (2017). "Requirement of Gamma-Carboxyglutamic Acid Modification and Phosphatidylserine Binding for the Activation of Tyro3, Axl, and Mertk Receptors by Growth Arrest-Specific 6." Front Immunol. **8**.

66. ^Munoz LE, et al. (2007). "The role of annexin A5 in the modulation of the immune response against dying and dead cells." Curr Med Chem. **14**(3):271-7.

67. a, bKang TH, et al. (2020). "Annexin A5 as an immune checkpoint inhibitor and tumor-homing molecule for cancer treatment." Nat Commun. **11**:1137.

68. ^Beck AW, et al. (2006). "Combination of a monoclonal anti-phosphatidylserine antibody with gemcitabine strongly inhibits the growth and metastasis of orthotopic pancreatic tumors in mice." Int J Cancer. **118**(10):2 639-43.

69. ^DeRose P, Thorpe PE, Gerber DE (2011). "Development of bavituximab, a vascular targeting agent with im mune-modulating properties, for lung cancer treatment." Immunotherapy. **3**(8):933-44.

70. ^He J, et al. (2009). "Antiphosphatidylserine antibody combined with irradiation damages tumor blood ves sels and induces tumor immunity in a rat model of glioblastoma." Clin Cancer Res. **15**(22):6871-80.

71. ^Frey B, et al. (2009). "AnnexinA5 renders dead tumor cells immunogenic--implications for multimodal ca ncer therapies." J Immunotoxicol. **6**(4):209-16.

72. ^Vuckovic S, et al. (2017). "The cationic small molecule GW4869 is cytotoxic to high phosphatidylserine-exp ressing myeloma cells." Br J Haematol. **177**(3):423-440.

73. ^Phinney NZ, et al. (2024). "Development of betabodies: The next generation of phosphatidylserine targetin g agents." Journal of Biological Chemistry. **300**(9).

74. ^Krais JJ, et al. (2017). "Antitumor Synergism and Enhanced Survival with a Tumor Vasculature-Targeted E nzyme Prodrug System, Rapamycin, and Cyclophosphamide." Mol Cancer Ther. **16**(9):1855-1865.

75. ^N'Guessan KF, Patel PH, Qi X (2020). "SapC-DOPS - a Phosphatidylserine-targeted Nanovesicle for selectiv e Cancer therapy." Cell Commun Signal. **18**(1):6.

76. ^Matharage JM, et al. (2015). "Unbiased Selection of Peptide-Peptoid Hybrids Specific for Lung Cancer Com pared to Normal Lung Epithelial Cells." ACS Chem Biol. **10**(12):2891-9.

Supplementary data: available at https://doi.org/10.32388/TMAXT9

Declarations

Funding: No specific funding was received for this work.

Potential competing interests: No potential competing interests to declare.